SUBSTRUCTURAL MODAL IDENTIFICATION OF LARGE SYSTEMS

LONG QUAN

NATIONAL UNIVERSITY OF SINGAPORE

2006

SUBSTRUCTURAL MODAL IDENTIFICATION OF LARGE SYSTEMS

LONG QUAN

(***B.Eng. TianJin University***)

A THESIS SUBMITTED

FOR THE DEGREE OF MASTER OF ENGINEERING

DEPARTMENT OF CIVIL ENGINEERING

NATIONAL UNIVERSITY OF SINGAPORE

2006

ACKNOWLEDGEMENT

Firstly, I would like to thank National University of Singapore for providing me a research scholarship and giving me such a great chance to pursue my research in Singapore.

Secondly, I would like to thank my supervisors, Professor Koh Chan Ghee and A/P Choo Yoo Sang for their useful advice and continuous guidance throughout my graduate study at the Department of Civil Engineering, NUS.

Thirdly, I thank all my fellow graduate students in Structural Engineering Group for many useful discussions.

Last but not least, I owe my thanks to my parents and all my friends, for their help and kind encouragement.

TABLE OF CONTENTS

SUMMARY

Model validation, updating and monitoring of large structures subjected to dynamic loading have been a subject of study for the last three to four decades. Monitoring of change of structural parameters during operation or after natural disasters (e.g. earthquake and storm) with satisfactory accuracy is needed to address safety concerns.

Non-classical methods based on biological concept, e.g. neural network, genetic algorithm, have been introduced into the domain of structural system identification. These methods are more robust and accurate than many classical identification methods on large structures. Nevertheless, when the number of degrees of freedom (DOFs) is substantial as in real structures, e.g. space truss system, even non-classical methods face difficulties converging or the amount of computational time required is prohibitive. To this end, it is necessary to constrain the number of degrees of freedom (DOFs). In this study, two recently developed methods are combined together, dividing the system physically and decoupling the system into modal domain. Several numerical examples are used to test the proposed method. In all these examples, structural stiffness parameters are regarded as unknowns. Though identification results on damping parameters are included in the last example, it is not the main purpose of this study. The first example is a 50 DOF lumped mass system, which is divided into 10 substructures for identification. The second example is a long span truss where a substructure is identified. The third example is a 400-DOF lumped mass system. A substructure of 35-DOF is identified. Furthermore, a frequency domain strategy aimed

at identifying offshore platforms is proposed. A 5 DOF substructure under mean sea level within a multiple DOF offshore platform is identified using the proposed substructural modal identification method. Up to 10% noise is considered in all examples. Measurement availability considered include 1/4, 1/2, 3/4 and full measurement.

The results of numerical simulation show that proposed approach is reasonably accurate and robust, and is considerably fast in solving large DOF system identification problem. Several aspects, including measurement unavailability, criteria optimization for the purpose of identifying damping parameters accurately, nonlinear phenomenon of structural model and experimental verification, are recommended for future research.

NOMENCLATURE

dA	area per length
a, b	Raleigh damping coefficients
C	damping matrix
$\mathbf{C}_{rr}$	damping matrix of substructure
C_{A}	added mass coefficient
C_{D}	drag coefficient
C_{M}	inertial coefficient
H	transfer function
H_s	significant wave height
K	stiffness matrix
$\mathbf{K}_{rr}$	stiffness matrix of substructure
K_n^*	modal stiffness of n-th mode
k_m	wave number
M	mass matrix
$\mathbf{M}_{rr}$	mass matrix of substructure
M_n^*	modal mass of n-th mode
p	probability density distribution function
P	force vector
$\mathbf{P}_r$	force vector of substructure
P_n^*	modal force of n-th mode
S_{xx}	power spectrum of structural displacement

$S_{\eta\eta}(\omega_m)$	power spectrum value corresponding to ω_m
t	time
Tp	peak period
ü , u̇ , u	acceleration vector, velocity vector and displacement vector
$\ddot{\mathbf{u}}_r, \dot{\mathbf{u}}_r, \mathbf{u}_r$	acceleration vector, velocity vector and displacement vector within substructure
$\ddot{\mathbf{u}}_j$ $\dot{\mathbf{u}}_j$ $\mathbf{u}_j$	acceleration vector, velocity vector and displacement vector at interface of substructure
u_r^s	quasi-static displacement
dV	column per length
$\ddot{Y}_n, \dot{Y}_n, Y_n$	modal acceleration, modal velocity and modal displacement of n-th mode
$\ddot{\mathbf{Y}}_{rn}^{*(m)}$	measured modal acceleration of n-th mode of substructure
$\ddot{\mathbf{Y}}_{rn}^{*(e)}$	estimated modal acceleration of n-th mode of substucture
Φ_n	n-th mode shape vector
ε	convergence tolerance
θ_{mn}	random phase angle of wave component
ω_m	wave frequency
α_{mn}	wave amplitude
$\Delta\omega$	frequency interval
η	wave elevation

LIST OF FIGURES

LIST OF TABLES

CHAPTER 1 INTRODUCTION

1.1 Background knowledge

Research in structural identification attracts much attention in recent years. Its applications include non-destructive health monitoring and damage detection. Through structural identification method, changes in structural parameters can be detected during operation or after natural disasters (e.g. earthquake and hurricane). Meanwhile, structural identification presents a challenging problem particularly when the system involves a large number of unknown parameters as in the real world. Besides accuracy and efficiency, robustness is an important issue for selecting an appropriate identification strategy. The following factors are often considered in numerical simulation study to test the effectiveness of the identification strategy.

(1) The strategy should not require unreasonably good initial guess for convergence.

(2) While accurate measurements are possible due to advances in sensor technology, inevitable noise affects the identification accuracy. The strategy should thus be tested in the presence of input and output (I/O) noise.

(3) Though more measurements give better results in general, the strategy should not assume complete measurement since this is difficult to achieve in reality.

(4) Dynamic response is normally measured by accelerometers. Error is incurred to obtain velocity and displacement signals by integration. Hence, direct use of acceleration signals is preferred over velocity and displacement signals.

When faced with large structural systems (in literature a structural system with more than 50 DOFs can be deemed as large system) with many unknown parameters, classical methods become numerically ill conditioned and convergence becomes difficult if not impossible. In this respect, heuristic strategies such as genetic algorithm (GA) and neural network are promising for structural identification. Unlike classical methods, heuristic strategies do not necessarily have mathematical basis but rely on simple rules and sheer computational power made possible only recently by rapid advances in computer technology.

1.2 Literature Review

1.2.1 Classical Methods

Classical methods are those built on rigorous mathematical foundation as opposed to those based on some heuristic rules such as evolutionary principles. Many classical methods has been proposed such as least square method, maximum likelihood method, extended Kalman filter method, Monte Carlo filter, etc. Some of these methods are described briefly as follows.

1.2.1.1 Recursive Least-Square

Caravani et al. (1977) carried out structural system identification based on recursive least-square method. The recursive least square method treats the unknown parameters as the solution vector in an equation set like direct least square method do. However, the criterion function is defined as the sum of squared errors between the estimated output and the measured output at every time step. Thus it relieves the computational burden caused by inverse operation of large matrix. The main advantage of this method is that it is relatively easy to implement. However, because measurement noise is not included in the formulation, identified results are biased by noise contamination in measurement signals.

1.2.1.2 Maximum Likelihood Method

This is a probability based approach in parameter estimation. Because all the estimated parameters are treated as random variables logically, it is justifiable to determine unknown parameters by maximizing the likelihood of matching the estimated responses with the measured response. This method is more advanced than least square method because the effect of noise is taken into consideration. However, it requires large amount of computing time and derivatives are also needed. In addition, the results are sensitive to the initial guess of the parameters.

1.2.1.3 Extended Kalman Filter

System dynamic equation can be formulated as a set of state space equations. Extended Kalman Filter (EKF) is modified by incorporating the parameters to be identified into the state vector and applied to parameter identification. In EKF method state variables are identified by updating state variables in time based on the system equations and next updating state variables based on measurements. The ideas of state estimation by Kalman filter for system identification was illustrated in Carmichael's work (Carmichael 1979). Yun and Shinozuka (1980) employed two filtering algorithms, namely the EKF and the iterated linear filter-smoother, to identify the hydrodynamic coefficient matrices of an offshore structure. Hoshiya and Saito (1984) developed an algorithm incorporating a weighted global iteration. Hoshiya and Maruyama (1987, 1991) identified parameters for a hysteretic restoring system and time-varying coefficient matrices using the EKF-WGI method. Loh and Tsaur (1988) applied the same method to identify an equivalent linear system, a bilinear hysteretic restoring system and a system with stiffness degradation effect. Yun et al. (1988) estimated structural parameters of a damaged bridge structure by the EKF. However, the main drawback of EKF is that the initial guess has to be within the vicinity of actual solution for good convergence.

1.2.1.4 Monte Carlo Filter (MCF)

Structural parameters are identified in this method by estimating recursively the conditional distribution function of the state variable when observation values up to the present time step are given. The distribution function of a state vector is described by many samples instead of first and second moments, unlike in the case of EKF. Therefore, the MCF has an advantage that it can deal with nonlinear and non-Gaussian noise problem. The applications of this method and its variation for system identification can be found in several recent works (Kitagawa 1996, Sato and Kaji 2000, Yoshida 2000).

1.2.1.5 Substructural Identification Method

Though many classical methods are available for structural identification, most works have considered small systems in the numerical examples presented. The recent trend of research is towards identification of large systems with many unknown parameters. For large systems, the main challenge is the computational efficiency to achieve reasonable accuracy of identified results within reasonable computational time.

Treating identification as an inverse problem, many classical methods of structural identification tend to be ill-conditioned numerically and hence the convergence becomes more difficult as the number of unknown parameters increases. A novel

strategy is to reduce the order of search domain by decomposing the structural system into smaller substructural systems. Koh et al. (1991) were the first to formulate a substructural identification method. Subsequent research works adopting the substructural approach include those by Oreta and Tanabe (1994), Yun and Lee (1997), Herrmann and Pradlwarter (1998) and Yun and Bahng (2000). In another attempt towards reducing computational time and difficulty, Koh et al. (1995) developed an improved condensation method suitable particularly for multi-story frame buildings.

1.2.2 Non- Classical Methods

When faced with large and complex structural system, classical methods become numerically ill-conditioned and the convergence tends to be extremely difficult.

As the power of digital computer grows tremendously, heuristic strategies, such as genetic algorithm and neural network, have been applied in structural system identification in past decades. Different from classical methods which are derived from mathematical principles, non-classical methods are based on heuristic rules and form the basis of artificial intelligence.

1.2.2.1 Neural Network

Neural network imitates the structure and working principle of humane brain. An artificial neural network is a system with input and output, composed of a number of

similar linear/nonlinear processing elements. These processing elements operate in parallel and are arranged in patterns similar to the patterns found in biological neural nets (Chassiako and Masri 1996). Adjustable weights, used to connect the processing elements with each other, are iteratively updated by a training algorithm. A key characteristic of neural networks is the capability of self-organisation or knowledge "learning". This self-organization capability allows automatic determination of the weights from the data containing the knowledge to be extracted to solve specific problems.

In the context of structural identification, unknown parameters can be recognized from given measurements by self-organization, avoiding comprehensive inverse analysis. The primary advantage of the artificial neural network methods is that they can potentially cope with challenging problems of robustness, complex nonlinear system and on-line identification (Kosmatopoulos and Polycarpou 1995, Chassiakos et al. 1998). The disadvantage is that only mathematical model, which may not have physical meaning (except for suitably constructed one-layer model), can be extracted. For damage identification, training data include input and output of the undamaged ("healthy") structure as well as the damaged structures. Wu et al. (1992) applied neural networks to identify damage of a simple three-storey frame by comparison of parameters of the "healthy" and damaged structures. Yun and Bahng (2000) applied the neural network to assess the damage locations and severities. The ratio of the resonant frequency before damage to the ones after is used as training data. The mode shape

after damage and the element stiffness index denote the damage location and extent. Chassiakos and Marsri (1996) applied neural network to process the non-parametric identification so that the responses are predicted by the mathematical model instead of the physical model of the system. However, this approach requires enough training information in order to perform well.

1.2.2.2 Genetic Algorithm

Genetic algorithm (GA) is by now a well-known non-classical optimization method. This approach imitates evolution of living things by natural selection, whereby parent genes combine and mutate to produce offspring by random variation, and compete based on the principle of "survival of the fittest". A good reference on the usual form of GA may be found in Goldberg (1989).

Exploration of search space and exploitation of good solution are two important issues in optimization approach. Hill-climbing is an example of a strategy which exploits the best solution for possible improvement while ignoring the exploration of search space. On the other end of the spectrum, random search is a strategy that explores the search space while ignoring exploitation of earlier solutions. Genetic algorithms are a class of general-purpose search methods providing a remarkable balance between exploration and exploitation.

The GA approach starts with an initial set of solutions called population. Each

individual in population is called a chromosome, representing a set of trial parameters. The chromosomes within the population with stronger fitness are identified and preferred in the selection. The new generation is derived by selection, mutation and crossover on the previous parent chromosomes.

In the context of *structural identification*, relatively few studies based on GA have been reported. Doyle (1994) used GA to identify the location of impact load and extended the study to identify location and size of transverse cracks in a beam (Doyle 1995). Dunn (1998) employed GA to identify a simple finite element model. Chou and Ghaboussi (2001) used GA to detect structural damage through static measurements. All numerical examples in the above-mentioned references are concerned with relatively simple structures with few degrees of freedom (DOFs) and few unknowns. But GA becomes very time consuming when the structure involves large numbers of DOFs and unknowns.

1.3 Proposed Strategy

Structural identification is essentially an optimization problem which aims to minimize the errors in some way when identifying unknown structural parameters, assuming that the structural model is well defined. In this connection, the genetic algorithms (GA) approach is well suited in structural identification owing to its versatility, robustness

and straightforward implementation as an optimization tool. Nevertheless, when it is applied to large systems, direct use of GA is often very time consuming computationally, because of the large number of forward analysis required. Thus, keeping the system size small and managable for identification is crucial in realistic structural identification problems. To this end, Koh et al. (2000) formulated a method of modal GA identification by transforming measured I/O signals in the physical domain to the modal domain and presented a fairly large system of 50 DOFs with good results. GA is used to identify modal parameters which are converted to physical parameters making use of the orthogonality properties of eigenvectors. This may be seen as a divide-and-conquer strategy, which greatly improves the identification effort by dealing with very few unknowns for each mode compared to identifying the whole system of many unknowns in the physical domain.

Another divide-and-conquer method based on GA to tackle large systems is the substructural identification approach proposed by Koh et al (2003a). Identification is conducted within each substructure with fewer parameters than identifying the whole structure. In addition, the identification efficiency is greatly improved since substructures can be identified independently and, if necessary, concurrently by means of parallel processing. Nevertheless, using either of these two divide-and-conquer strategies may not be sufficient for larger and more complex structures. In this study, these two divide-and-conquer strategies are combined. Formulation is presented, followed by numerical simulation study including identification of structure of many

DOFs based on incomplete and noisy signals. There are other strategies to tackle large systems. Parallel GA computing takes advantage of concurrency of GA. Some hybrid strategies (Koh et al 2003b, Perry et al 2006) are used to improve accuracy of identification by adding local search operators (modified GA). But these are not considered in this study to keep the scope manageable.

1.4 Objective and Scope of Research

To tackle system identification problem of very large structural system several strategies can be employed. Substructural method and modal GA strategy are divide-and-conquer methods which reduce DOFs of each identification run. This study aims at combining the two different divide-and-conque methods to provide an efficient, robust and accurate identification method for large structural system.

Chapter 1 presents background knowledge and general literature review of structural system identification, with regards to both classical and non classical methods.

In chapter 2, theoretical formulation of substructural modal method is proposed as a combination of substructural identification approach and structural modal identification, for the purpose of identifying large structures more efficiently.

Chapter 3 presents four numerical examples showing the advantage and potential application of this method. The first example is a 50-DOF lumped mass dynamic system. The second example is a long span truss of 57-DOFs. The third example is a very large structural system (400 DOFs) of which one large substructure is identified. In these examples, effects of incomplete measurement and contaminated signals are studied. In addition computational time is compared with direct GA and direct substructural method.

Chapter 4 demonstrates examples as an application to offshore platform identification which are conducted in frequency domain.

Chapter 5 concludes the research work and recommends topics for future research.

CHAPTER 2 SUBSTRUCTURAL MODAL IDENTIFICATION OF LARGE SYSTEM

2.1 Substructural Identification Method

For convenience, we consider a lumped mass structure as shown in Fig 2.1. The equation of motion of the substructure is expressed as

$$\begin{bmatrix}\mathbf{M}_{rj} & \mathbf{M}_{rr}\end{bmatrix}\begin{Bmatrix}\ddot{\mathbf{u}}_j(t)\\ \ddot{\mathbf{u}}_r(t)\end{Bmatrix}+\begin{bmatrix}\mathbf{C}_{rj} & \mathbf{C}_{rr}\end{bmatrix}\begin{Bmatrix}\dot{\mathbf{u}}_j(t)\\ \dot{\mathbf{u}}_r(t)\end{Bmatrix}+\begin{bmatrix}\mathbf{K}_{rj} & \mathbf{K}_{rr}\end{bmatrix}\begin{Bmatrix}\mathbf{u}_j(t)\\ \mathbf{u}_r(t)\end{Bmatrix}=\mathbf{P}_r(t) \tag{2.1}$$

where subscripts *r* and *j* denote internal DOFs and interface DOFs, respectively. The usual notations **M**, **C** and **K** denote mass, damping and stiffness matrices, respectively, and **P** denotes load vector. Treating interaction effects at the interface nodes as input forces, the above equation system can be re-arranged as

$$\mathbf{M}_{rr}\ddot{\mathbf{u}}_r(t)+\mathbf{C}_{rr}\dot{\mathbf{u}}_r(t)+\mathbf{K}_{rr}\mathbf{u}_r(t)=\mathbf{P}_r(t)-\mathbf{M}_{rj}\ddot{\mathbf{u}}_j(t)-\mathbf{C}_{rj}\dot{\mathbf{u}}_j(t)-\mathbf{K}_{rj}\mathbf{u}_j(t) \tag{2.2}$$

In practice, dynamic response is usually measured by means of accelerometers. Error is inevitably incurred when computing velocity and displacement signals by numerical integration. Hence, direct use of acceleration signals is preferred over velocity and

displacement signals. The concept of 'quasi-static displacement' is necessarily adopted in order to remove the displacement term in the RHS of equation (2.2), as follows.

$$\mathbf{u}_r(t) = \mathbf{u}_r^s(t) + \mathbf{u}_r^*(t) \tag{2.3}$$

where $\mathbf{u}_r^s = -\mathbf{K}_{rr}^{-1}\mathbf{K}_{rj}\mathbf{u}_j = \mathbf{r}\mathbf{u}_j$ is the quasi-static displacement. Thus equation (2.2), after neglecting interface damping force term which is relatively small in civil engineering structures, can be rewritten such that only accelerations at the interface are involved on the RHS as follows

$$\mathbf{M}_{rr}\ddot{\mathbf{u}}_r^*(t) + \mathbf{C}_{rr}\dot{\mathbf{u}}_r^*(t) + \mathbf{K}_{rr}\mathbf{u}_r^*(t) = \mathbf{P}_r(t) - (\mathbf{M}_{rj} + \mathbf{M}_{rr}\mathbf{r})\ddot{\mathbf{u}}_j(t) \tag{2.4}$$

Based on equation (2.4), GA can be used to identify the substructural parameters $\mathbf{M}_{rr}$, $\mathbf{K}_{rr}$ and $\mathbf{C}_{rr}$.

2.2 Modal GA Identification Method

The dynamic equation of an *N*-DOF system can be written in standard notation as follows:

$$\mathbf{M}\ddot{\mathbf{u}} + \mathbf{C}\dot{\mathbf{u}} + \mathbf{K}\mathbf{u} = \mathbf{P}(t) \tag{2.5}$$

where **M**, **C**, and **K** are mass, damping, and stiffness matrices, respectively; **u** is displacement vector; $\dot{\mathbf{u}}$ is velocity vector; $\ddot{\mathbf{u}}$ is acceleration vector; **P** is force vector and *t* is time. A commonly used proportional damping is assumed here as

$$\mathbf{C} = a\mathbf{M} + b\mathbf{K} \tag{2.6}$$

where *a* and *b* are damping constants which can be calculated from damping ratios of any two modes.

To reduce the number of unknowns, identification is conducted in each mode instead of identifying the physical parameters directly. The dynamic equation (2.5) can be decoupled as follow:

$$M_n^*\ddot{Y}_n + (aM_n^* + bK_n^*)\dot{Y}_n + K_n^*Y_n = P_n^*(t) \qquad n= 1, 2,\ldots N \tag{2.7}$$

where $M_n^* = \mathbf{\Phi}_n^T\mathbf{M}\mathbf{\Phi}_n$, $K_n^* = \mathbf{\Phi}_\mathbf{n}^\mathbf{T}\mathbf{K}\mathbf{\Phi}_n$, and $P_n^* = \mathbf{\Phi}_n^T\mathbf{P}$, $\mathbf{\Phi}_n$ is the *n*-th mode shape, Y_n is corresponding modal coordinate in time domain.

Based on equation (2.7), GA can be used to carry out identification of modal parameters in each mode. As explained before, acceleration is preferred over velocity and displacement as measurement. Thus, the fitness value in each mode is defined as

$$fitness_n = \sum_{l=1}^{L} \frac{1}{(\ddot{Y}_n^e(l) - \ddot{Y}_n^a(l))^2} \tag{2.8}$$

where L is the total number of time steps; $\ddot{Y}_n^e$ is the estimated modal acceleration response by solving equation (2.7); $\ddot{Y}_n^a$ is the actual modal acceleration response calculated from $\mathbf{\Phi}_n^T \mathbf{M} \ddot{\mathbf{u}}^a / M_n^*$, superscript a denote actual acceleration. After identifying the modal property, physical parameters are recovered by means of orthogonality equations. With the improved physical parameters, eigenvalue analysis is carried out again and the procedure is repeated until convergence.

2.3 Proposed Substructural Modal Identification Method

In this section, the two divide-and-conquer methods, i.e. modal GA method and substructural identification method are ingeniously combined together. Transforming physical time signals as defined in equation (2.3) into modal coordinates gives

$$\mathbf{u}_r(t) = \mathbf{\Phi}_r(\mathbf{Y}_r^s(t) + \mathbf{Y}_r^*(t)) \tag{2.5}$$

where $\mathbf{\Phi}_r$ is the matrix of eigen vectors (mode shapes) of the substructural dynamic system and $\mathbf{Y}_r^s$ is defined as $\mathbf{\Phi}_r{}^{-1}\mathbf{r}\mathbf{u}_j$. Modal acceleration is thus given by

$$\ddot{\mathbf{Y}}_r^* = \mathbf{\Phi}_r{}^{-1}(\ddot{\mathbf{u}}_r - \mathbf{r}\ddot{\mathbf{u}}_j) \tag{2.6}$$

Equation (2.4) can be transformed into the modal domain as

$$M_{rrn}\ddot{Y}^{*}_{rn}(t) + C_{rrn}\dot{Y}^{*}_{rn}(t) + K_{rrn}Y^{*}_{rn}(t) = \mathbf{\Phi}^{T}_{rn}(\mathbf{P}_{r}(t) - (\mathbf{M}_{rj} + \mathbf{M}_{rr}\mathbf{r})\ddot{\mathbf{u}}_{j}(t)) \qquad (2.7)$$

where subscript n denotes the eigen-mode number of the substructure, and the corresponding modal properties are given by $M_{rrn} = \mathbf{\Phi}^{T}_{rn}\mathbf{M}_{rr}\mathbf{\Phi}_{rn}$, $C_{rrn} = \mathbf{\Phi}^{T}_{rn}\mathbf{C}_{rr}\mathbf{\Phi}_{rn}$, $K_{rrn} = \mathbf{\Phi}^{T}_{rn}\mathbf{K}_{rr}\mathbf{\Phi}_{rn}$.

For the substructure concerned, proportional damping matrix is adopted. Hence,

$$\mathbf{C}_{rr} = a\mathbf{M}_{rr} + b\mathbf{K}_{rr} \qquad (2.8)$$

where a and b are two damping constants which are treated as unknowns to be determined by damping ratios of any two modes of the substructure.

The actual modal acceleration is obtained through

$$\ddot{Y}^{*(a)}_{rn} = \mathbf{\Phi}^{T}_{rn}\mathbf{M}_{rr}(\ddot{\mathbf{u}}_{r}^{(a)} - \mathbf{r}\ddot{\mathbf{u}}_{j}^{(a)}) / M_{rrn} \qquad (2.9)$$

The difference between the estimated modal acceleration (numerically obtained based on Eq. 2.7) and the measured modal acceleration is used in defining the fitness value

as required in GA. Specifically the GA aims to maximize the fitness defined as:

$$fitness_n = \frac{1}{\sum_{t=1}^{L} (\ddot{Y}_{rn}^{*(a)}(t) - \ddot{Y}_{rn}^{*(e)}(t))^2} \tag{2.10}$$

where L is the number of time steps used in the time history, and superscripts *e* and *a* denote the modal acceleration responses corresponding to the estimated system and the actual system, respectively.

With the estimated eigenvalues and eigenvectors, physical parameters can be recovered by exploiting the orthogonality properties of the eigen vectors. This recovery process leads to an over-determined system of equations which can easily be solved by the least-squares method (Koh et al 2000).

The above procedure assumes that the acceleration signals at all internal DOFs are available, which is very difficult to achieve in reality. This problem is easily resolved since the proposed method is iterative in nature as illustrated in Fig. 2.2 and allows improvement to be made for any assumed response. For instance, if the acceleration signal at the *i*-th internal DOF is not measured, this can be iteratively updated by a simple scaling based on the acceleration signal measured at the *k*-th internal DOF (the nearest measured node should be used for good accuracy), as follows

$$\ddot{\mathbf{u}}_i^{(a)} = \ddot{\mathbf{u}}_k^{(a)} \ddot{\mathbf{u}}_i^{(e)} / \ddot{\mathbf{u}}_k^{(e)} \tag{2.11}$$

A convergence tolerance is required to end the iterations. Convergence is deemed achieved when the mean of the relative differences between the identified stiffness coefficients of the current (j-th) iteration and the previous iteration is less than the specified tolerance (ε), as follows:

$$\frac{1}{N} \sum_{i=1}^{N} \frac{| k_i^{(j)} - k_i^{(j-1)} |}{k_i^{(j-1)}} < \varepsilon \tag{2.12}$$

The fitness values of all sets of recovered physical parameter are calculated. Upon convergence or sufficient iterations the set with the highest fitness value is deemed to be the identified set.

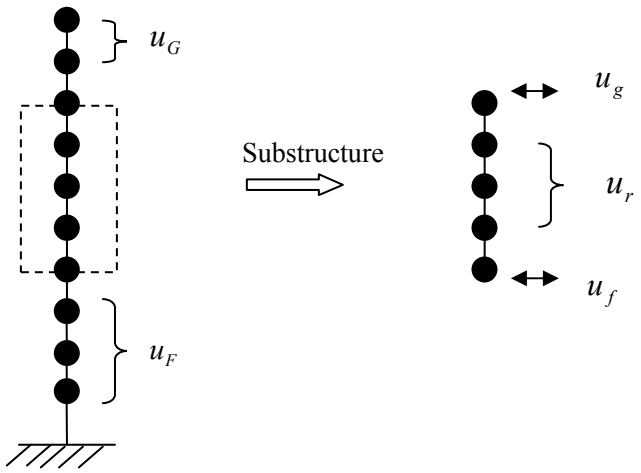

Fig.2.1 Complete Structure and Substructure

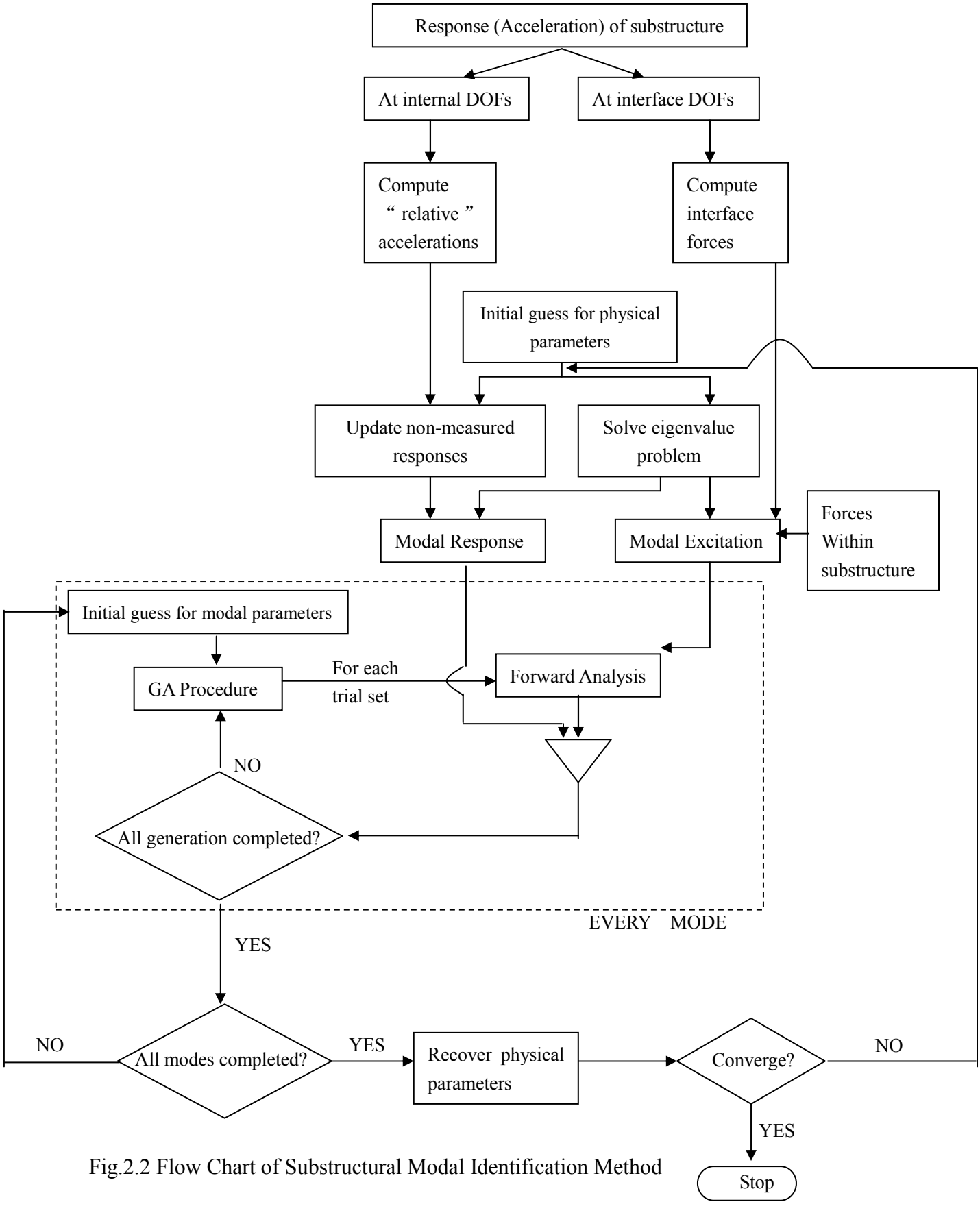

Fig.2.2 Flow Chart of Substructural Modal Identification Method

CHAPTER 3 NUMERICAL SIMULATION STUDY

3.1 General Remarks

In order to evaluate the performance of the proposed method, numerical simulation study is carried out on the identification of three fairly large structural systems with known exact parameters. Incomplete measurement (simulated) is considered with noise (5% and 10%) added to the I/O signals. In the first example, a 50-DOF lumped mass system is considered and the whole structure is identified by having ten substructures. In the second example, a substructure in a long-span truss structure is identified. The third example is a 400-DOF lumped mass system. A substructure of 35-DOF is identified. In all the examples, Rayleigh damping is adopted to account for energy dissipation in the structures and modal damping ratios are taken as 5%. Applied forces are random excitation in the form of Gaussian white noise and taken as measured with noise (5% and 10%). The measurement signals are obtained for 1000 time instants at 0.01s time interval using Newmark's constant-acceleration method (Bathe 1996).

3.2 Identification of 50-DOF Lumped Mass System

Consider a 50-DOF lumped mass system as shown in Fig 3.1. The exact mass is 600 kg for the first mass and 300 kg for the others. The exact stiffness value is 700 kN/m at all levels. Random forces are applied on the 3rd, 8th, 13th, 18th, …, 48th levels. The proposed method is applied by dividing the whole structural system into ten substructures as [0-5], [5-10], [10-15], …, [45-50], where node 0 represents the ground node (fixed), 1 the lowest level and 50 the highest level. In each substructure, there are four internal nodes. Except for the first and the last substructures, each substructure has two interface nodes. GA population size of 50 is found to be sufficient to carry out the identification task.

(a) Effects of incomplete measurement

To study the effects of incomplete measurement, the following scenarios are considered. Signals are not contaminated with noise.

(1) Complete measurement: The accelerations at all internal DOFs in each substructure are known.

(2) 3/4 measurement: The accelerations of the 2nd, 3rd and 4th nodes in each substructure are known.

(3) 1/2 measurement: The accelerations of the 2nd and 3rd nodes in each substructure are known.

(4) 1/4 measurement: The acceleration of the 3rd node in each substructure is

known.

The identification stiffness values in terms of the ratios to the exact values are presented in Figs. 3.2 to 3.5 for the above scenarios. The mean absolute errors of identified stiffness parameters are summarised in Table 3.1. As expected, the accuracy declines gradually with the availability of lesser measurements. Nevertheless the identified results are still reasonably good with mean error of about 6% even for 1/4 measurement where only the acceleration at one internal node is available. For comparison purpose, the GA method is also applied to the complete structure in a direct manner, referred to as the "complete structural identification" method. The identified results based on this method are considerably poorer, as presented in Fig. 3.6.

(b) Effects of I/O noise

Real world signals are inevitably contaminated with noise. To study the effects of I/O noise, the time histories of excitations and responses are artificially contaminated with zero-mean white Gaussian noise. The noise level is defined as the ratio of standard deviation of the noise to the root-mean-square value of the uncontaminated time history. Two noise levels, i.e. 5% and 10%, are considered for the scenarios of 1/4 measurement and 1/2 measurement. The identified results are presented in Table 3.2. The mean absolute error of the identified results is about 9% for 5% noise level and about 14% for 10% noise level, using the proposed method with

only 1/4 measurement. The results are considered good in view of the incomplete measurement with noise.

In this example, the proposed method has little advantage over substructural method in terms of computational time, since the number of DOFs contained in each substructure is very small.

3.3 Identification of Long Span Truss System

A substructure of a long span truss structure considered by Koh et al (2003) is to be identified. The statically indeterminate structure comprises 57 truss members (57 DOFs) as shown in Fig. 3.8. The exact values for all truss members are Young's modulus, E = 200 GPa (steel) and cross sectional areas, A = 0.0015 m^2. The substructure of interest comprises 11 members with unknown EA values. To account for damping, two Rayleigh damping constants for the substructure are included as unknown. Three internal accelerations (a_1, a_2 and a_3 as shown in Fig. 3.9) are measured, in addition to all interface accelerations. The whole structure is subjected to eight random forces (F_1 to F_8), but only F_3 and F_4 within the substructure are required by the proposed method since the other six forces are outside the substructure of concern. In this regard, it should be stressed that the identification of this substructure does not required any information of force, response, size, geometry or

support conditions of the remainder of the structure.

Identification is carried out twice with different initial populations which are randomly generated using the search range of 0.5-2 times the exact value. Based on the average of the two sets of identified parameters, the mean absolute error for noise free case is 5.72% as presented in Table 3.3. Next, the I/O signals are contaminated with 10%. The corresponding mean absolute error is 9.65% which is very good in view of the high noise level.

3.4 Identification of 400-DOF Lumped Mass System

A substructure of 35 DOFs in a lumped mass system of 400 DOFs is identified as shown in Fig 3.10, which is the largest structure being identified in the author's knowledge. The exact stiffness is 700 kN/m for each level, while the mass is 600 kg for the first level and 300 kg for others. A proportional damping matrix is assumed the same with Example.1. A total of 80 excitations as white noise, are assumed to apply at 3^{rd}, 8^{th}, 13^{th},…, 398^{th} levels. The prohibitive computational cost makes it impractical to identify this large system of 400 DOFs by the complete substructural method (Koh et al. 2003). To this end, the fast convergence of the proposed method makes identification of this large system possible. Stiffnesses of the substructure from 1^{st} level to 35^{th} level were identified. Acceleration response is available at every five

nodes, i.e. 3rd, 8th, 13th, 18th, 23rd, 28th, 33rd, and 35th, the interface, in the substructure. The initial values are randomly generated in a range between 450 KN/m and 1400 KN/m (the lower and upper bound), which are 64% and 200% of the true value respectively.

Two levels of I/O noise are considered: 5% and 10%. As shown in Table 3.4, absolute mean errors of the identified results are, respectively, 6.99% and 11.48% in 5% and 10% noise cases. All the examples were ran on a computer with CPU configured as Intel(R) Pentium (R) M Processor 1500 MHz 1.50 GHz. CPU time in both cases is 1694s and 3297s. For comparison, the absolute mean error and CPU time of substructural method without noise are 11.23% and 10393 s respectively. Compared with the results obtained by the substructural method for 0% noise, it is clear that the substructural modal identification is much more efficient and accurate.

3.5 Observation on Maximum Error

In Fig 3.3, the points where highest error occurs in each substructure are marked with circles of dashed line. The points where no measurements are taken are marked with circles of real line. It is observed that they normally do not coincide with each other. The location of maximum error in each substructure is randomly distributed, which can also be noticed in other scenarios of incomplete measurement.

Maximum errors in Table 3.1-3.3 normally have values approximately 3 times as big

as corresponding absolute mean error. It is difficult to control the maximum error in this study due to the probabilistic nature of GA. The strategy of maximum error controlling, which involves local search operators, is out of the scope of this thesis.

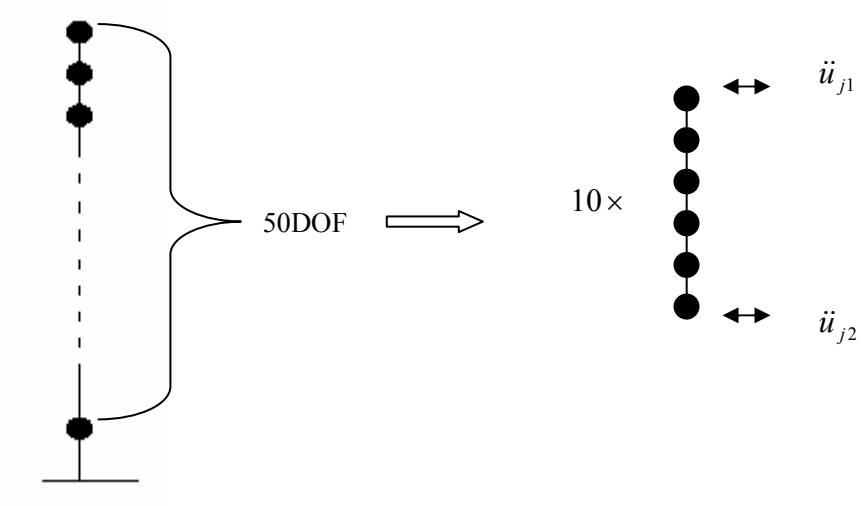

Fig.3.1 50-DOF Lumped Mass System

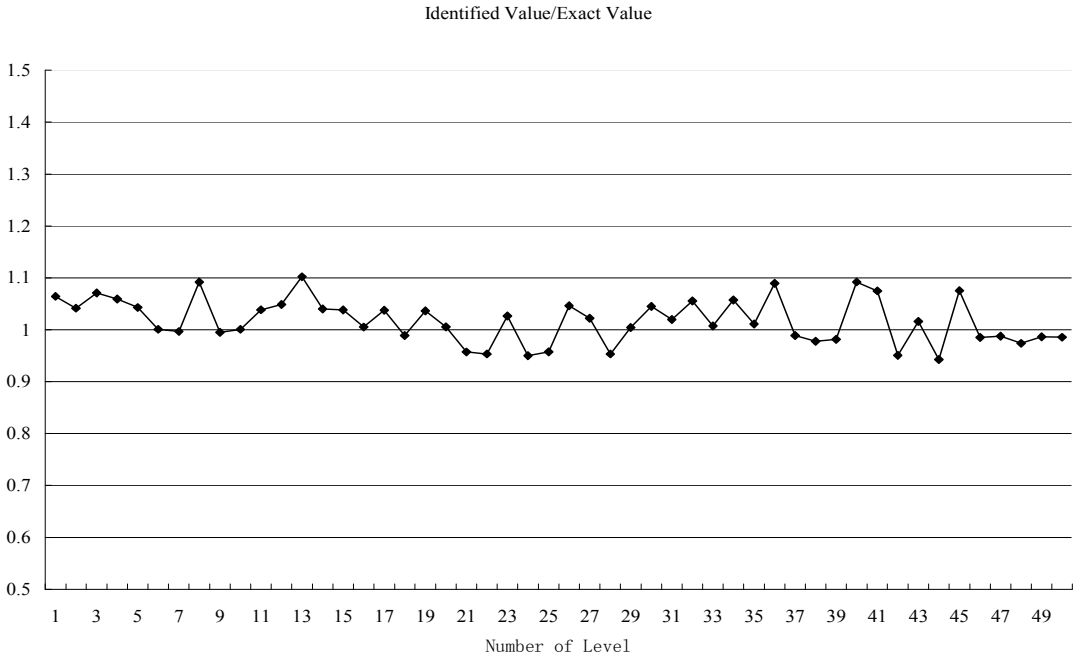

Fig.3.2 Result of Example 3.1 with Full Measurement

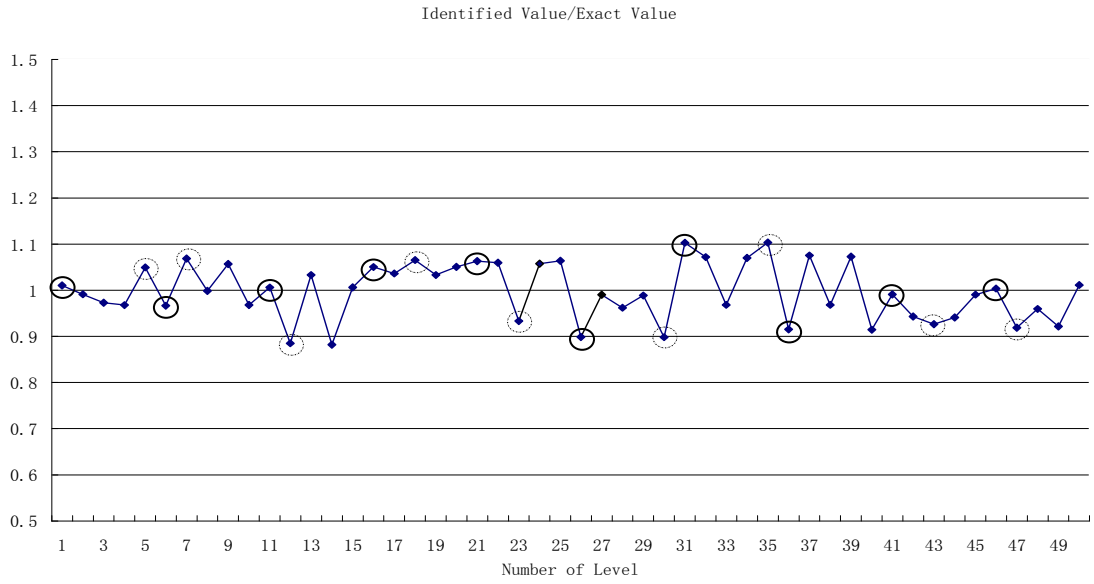

Fig.3.3 Results of Example 3.1 with 3/4 Measurements

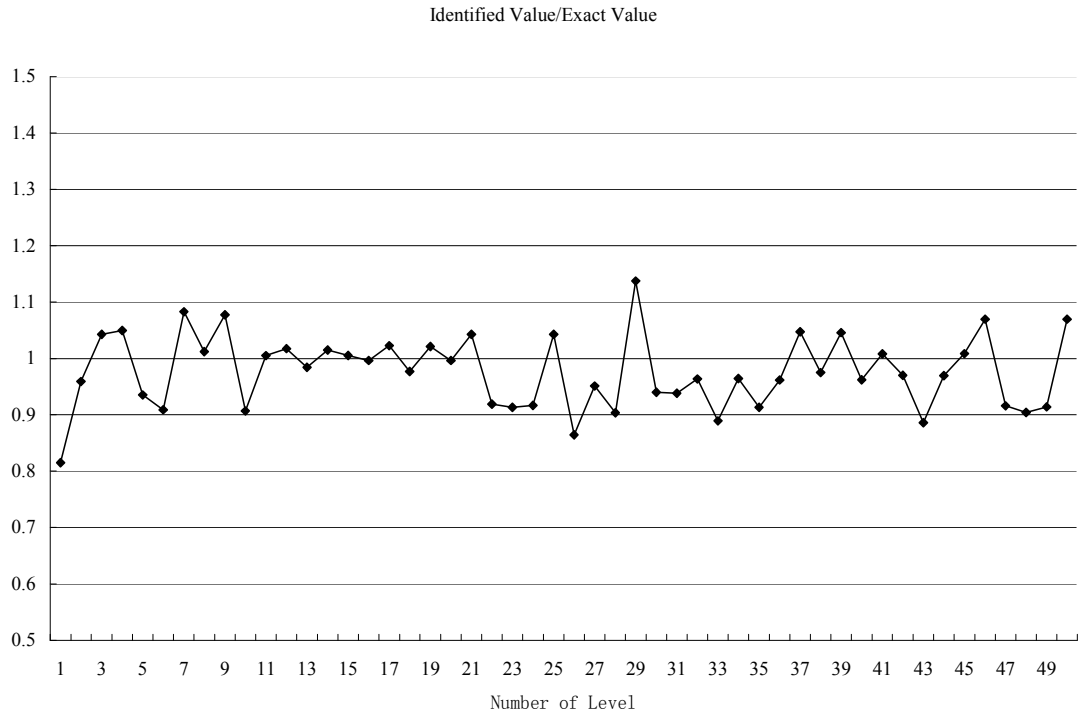

Fig.3.4 Results of Example 3.1 with 1/2 Measurements

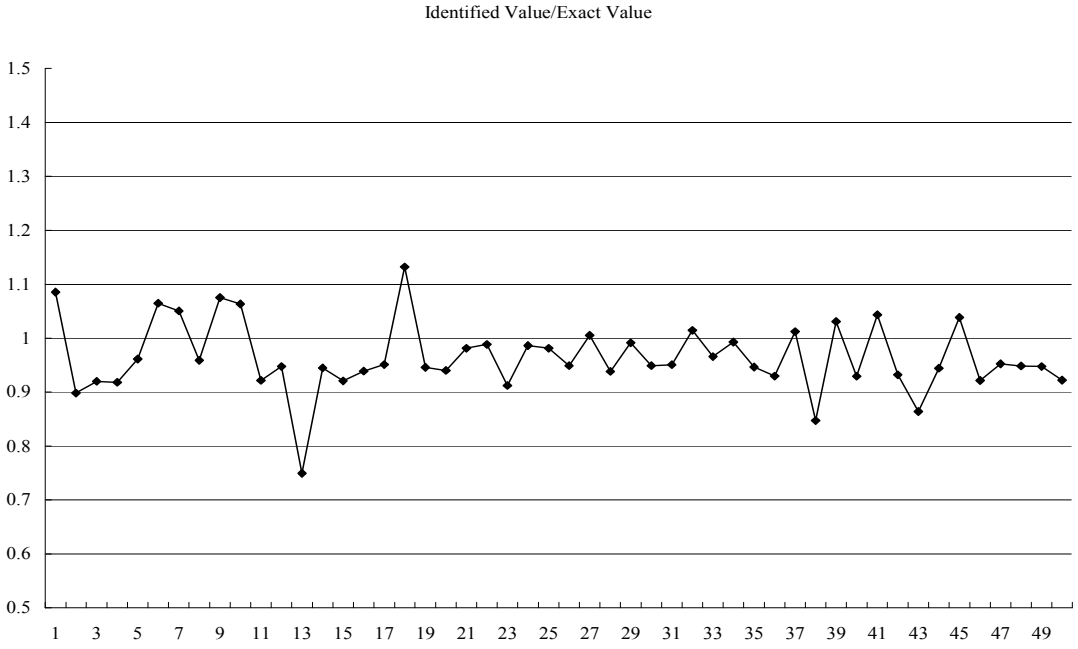

Fig.3.5 Results of Example 3.1 with1/4 Measurements

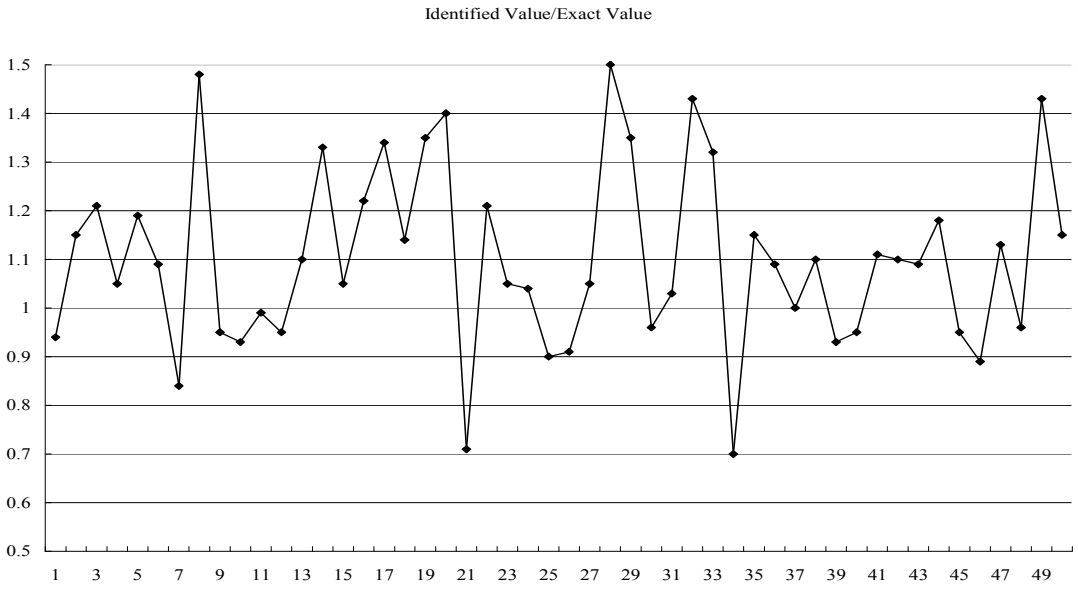

Fig.3.6 Results of Direct GA Method with Full Measurements

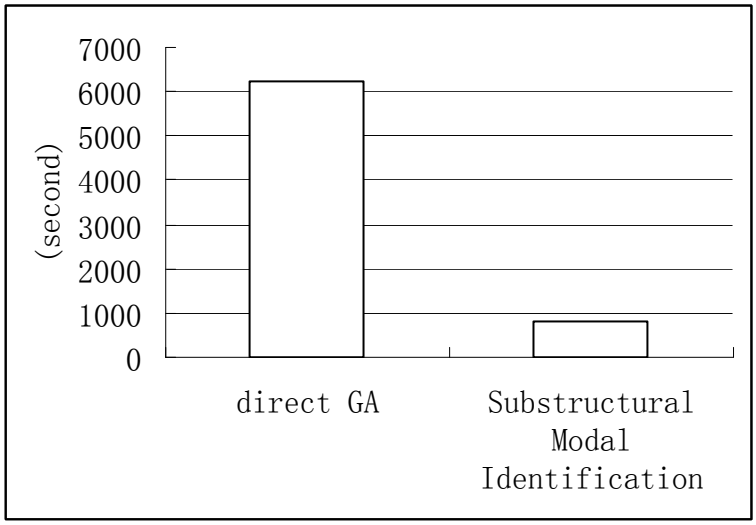

Fig.3.7 Comparison of Computational Time between Proposed Method and Direct GA Method

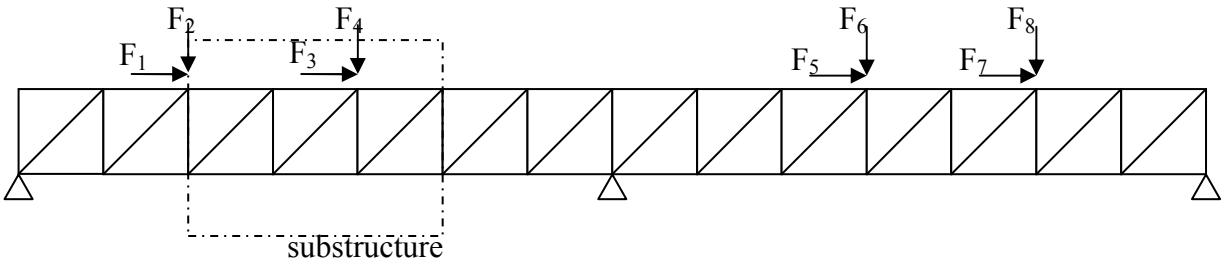

Fig.3.8 Long Span Truss Structure Model

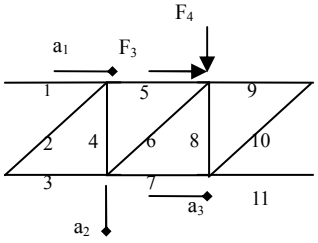

Fig.3.9 Substructure

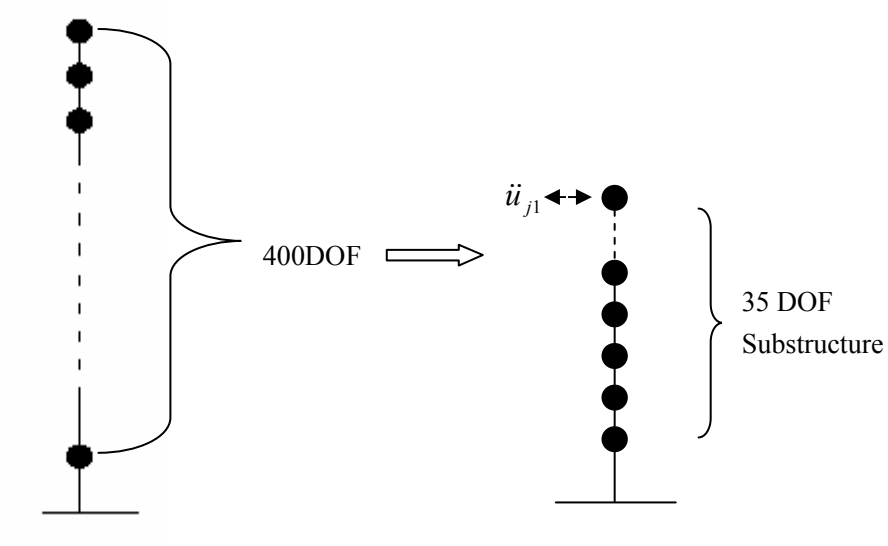

Fig. 3.10 400 DOF Lumped Mass System and the Substructure Identified

Table.3.1 Identified Results of Full Measurement and Incomplete Measurement Cases

	Full Measurement	3/4 Measurement	2/4 Measurement	1/4 Measurement
Mean error	3.70%	5.10%	5.61%	6.05%
Maximum error	10.20%	11.80%	18.50%	25.06%

Table.3.2 Identification Results of Noise Polluted and Incomplete Measurement

Number of Stiffness	Exact Value (KN/M)	5%noise 1/4 Measurement	10%noise 1/4 Measurement	5%noise 1/2 Measurement	10%noise 1/2 Measurement
1	700.00	682.06	635.50	677.12	662.11
2	700.00	731.86	835.31	763.82	717.15
3	700.00	644.56	717.08	695.58	684.60
4	700.00	652.16	959.77	655.74	745.55
5	700.00	786.25	585.40	781.46	721.69
6	700.00	634.05	713.56	726.18	686.81
7	700.00	688.05	863.16	764.51	637.84
8	700.00	935.50	624.22	833.65	703.62
9	700.00	684.00	807.22	759.32	634.98
10	700.00	635.47	700.60	725.47	687.66
11	700.00	731.99	512.66	767.85	746.49
12	700.00	688.73	628.73	782.85	728.80
13	700.00	636.72	665.35	783.28	769.00
14	700.00	692.06	627.09	780.83	726.82
15	700.00	733.46	514.03	767.94	743.27
16	700.00	668.93	560.68	734.47	799.78
17	700.00	631.97	802.23	642.93	754.03
18	700.00	610.38	618.42	637.76	771.72
19	700.00	630.57	799.25	660.51	732.65
20	700.00	668.58	560.19	731.47	795.58
21	700.00	820.04	499.64	708.70	827.41
22	700.00	833.43	644.84	743.62	727.18
23	700.00	930.46	547.36	814.54	841.24
24	700.00	772.47	659.29	740.51	794.91
25	700.00	853.62	511.60	709.16	852.26
26	700.00	788.41	436.58	767.20	823.48

27	700.00	775.43	948.83	782.46	697.71
28	700.00	864.48	605.27	759.03	631.11
29	700.00	770.25	948.51	782.42	698.58
30	700.00	789.04	436.94	765.53	825.20
31	700.00	701.13	699.90	711.70	578.83
32	700.00	751.64	835.01	769.85	820.19
33	700.00	785.56	624.83	793.28	696.26
34	700.00	745.59	806.17	749.75	786.34
35	700.00	701.44	703.35	702.93	629.00
36	700.00	680.20	650.07	682.19	744.93
37	700.00	738.86	649.73	702.76	729.95
38	700.00	659.87	584.43	686.65	783.88
39	700.00	734.27	626.81	704.72	754.63
40	700.00	680.02	629.61	679.29	758.45
41	700.00	603.34	675.36	782.58	701.84
42	700.00	734.98	761.35	846.44	627.70
43	700.00	822.08	762.45	760.42	788.30
44	700.00	705.26	747.64	847.89	626.13
45	700.00	617.24	669.87	803.45	701.95
46	700.00	718.76	668.13	651.61	636.96
47	700.00	734.95	599.08	709.88	700.35
48	700.00	681.73	687.54	634.58	614.70
49	700.00	722.83	593.91	697.62	701.22
50	700.00	724.23	669.87	647.18	637.90
Mean absolute error		8.76%	14.31%	7.22%	8.15%
Maximum absolute error		33.64%	37.63%	21.13%	21.75%

Table.3.3 Substructural Modal Identification of Truss Structure

Number of member	Exact EA(MN)	Identified EA(MN)	
		0 Noise	10%noise
1	300	272.433	269.818
2	300	292.544	300
3	300	267.665	238.484
4	300	284.182	327.155
5	300	292.342	325.457
6	300	293.013	328.748
7	300	292.632	325.491
8	300	284.797	327.228
9	300	267.652	238.483
10	300	291.506	300
11	300	272.579	268.982
Mean absolute error		5.72%	9.65%
Maximum absolute error		10.78%	20.50%

Table 3.4 Substructural Modal Identification of 400 DOF system

Number of Stiffness	Exact Value	Identified Value(5%noise)	Identified Value(10%noise)	Substructural Identification (no noise)
1	700.00	659.95	727.93	1030.78
2	700.00	771.08	791.12	812.79
3	700.00	714.29	710.43	852.70
4	700.00	672.78	749.18	637.33
5	700.00	742.57	598.17	845.16
6	700.00	709.77	657.93	629.96
7	700.00	688.42	799.16	741.05
8	700.00	740.85	763.29	726.96
9	700.00	725.47	686.38	677.08
10	700.00	761.91	723.74	813.27
11	700.00	795.93	802.97	820.37
12	700.00	704.74	545.71	646.62
13	700.00	779.82	736.00	672.94
14	700.00	631.32	542.59	712.99
15	700.00	800.74	670.38	723.55
16	700.00	652.00	631.74	858.74
17	700.00	647.98	831.02	840.73
18	700.00	778.90	530.25	604.47
19	700.00	749.83	793.78	817.40
20	700.00	623.66	864.79	844.87
21	700.00	597.46	871.52	760.02
22	700.00	782.71	801.10	774.12
23	700.00	636.81	678.53	706.57
24	700.00	657.73	699.40	767.72
25	700.00	733.90	599.88	641.61
26	700.00	654.72	750.22	688.01
27	700.00	693.53	637.01	678.80
28	700.00	608.60	861.03	734.49
29	700.00	802.55	779.32	783.85
30	700.00	717.38	669.18	635.92
31	700.00	683.93	785.59	788.63
32	700.00	703.25	618.78	642.03
33	700.00	665.12	678.97	768.67
34	700.00	685.91	851.68	643.56
35	700.00	642.44	764.16	725.58
	Absolute Mean Error	6.99%	11.48%	11.23%
	CPU Time	1693.875	3296.906s	10393.327 s

CHAPTER 4 SYSTEM IDENTIFICATION FOR OFFSHORE PLATFORMS

4.1 Introduction

Offshore structures play an important role in mankind's adventure in ocean. Most offshore structures, such as jacket and jack-up platforms used for oil exploration and production, have been intensely studied with regards to response prediction (forward analysis) in recent years.

Here we are looking at the offshore identification problem (inverse problem). The potential applications include structural health monitoring, structural model updating and calibration, and hydrodynamic force estimation by identifying the hydrodynamic coefficients.

Due to uncertainty in the hydrodynamic load estimation, dynamic analysis of offshore structures is still a challenging topic. Meanwhile, no time history of hydrodynamic force is measurable. Therefore, system identification method in time domain is not practical in offshore platform identification. In this chapter, a method based on power spectral density function is formulated.

4.2 Offshore Platform Forward Analysis in Time Domain

In practice, hydrodynamic forces imposed on the offshore rig cannot be measured directly. What can be measured is the wave elevations in certain locations. Wave kinematics is then derived based on appropriate wave theories, and wave forces are evaluated. Morison force is considered here because offshore platform is drag force dominant structure. Finally structural dynamic analysis is carried out. The procedure is illustrated in Fig.4.1.

The process mentioned in above paragraph is the most common approach used by researchers and engineers for modeling purpose. The method relies on solving the equations of motion of a 3D structural model of the jack-up at discrete time-steps under time-varying loading. In principle, almost all of the non-linear effects may be accounted for directly in the analysis. In particular, the wave loading requires no linearization, and the displaced position and relative motion of the structure may be accounted for if desired. The structural model may also be a fully non-linear system which is considerably more expensive in computer resources than the solution using a linear structure, as non-linear analysis requires the reformulation and decomposition of the stiffness matrix at each time-step. To obtain accurate results it is necessary to ensure that a sufficiently small time step is applied.

In offshore structural modeling, regular wave method and irregular wave method can

be used. However, it is felt that regular wave method cannot provide enough accuracy for parameter identification purpose. Only irregular wave method is adopted in this study.

The essential difference from the regular wave method is that the wave loading is now based on a random wave theory. This usually involves the superposition of number of first order (Airy) wave components at random phase. The amplitudes of the components are determined by dividing the wave spectrum into “slices” of either constant frequency increment or of constant energy content. The latter has the advantage that the definition in the region of highest wave energy will be more accurate. The component wave height at a particular frequency, representative of the slice, is computed so that the energy of the component matches that of the slice it represents.

The instantaneous free surface of the random sea is determined from the sum of the component wave heights at random phases. The asymmetry of the crest and trough heights, accounted for in higher order wave theories, is not seen in methods based on random waves. The particle kinematics from first order wave theory are computed assuming the wave height is small and hence the kinematics are only valid up to the mean water level.

The following equation is usually used to simulate a random sea wave elevation in

time domain:

$$\eta(x,y,t)=\sum_{n=1}^{N}\sum_{m=1}^{M}\alpha_{mn}\cos(k_m x\cos\phi_n+k_m y\sin\phi_n-\omega_m t+\theta_{mn}) \tag{4.1}$$

where x and y are two Cartesian coordinates, t is time, ϕ_n is wave propagation angle, k_m is wave number, and ω_m is the wave frequency (radium/second). In this equation describing 3-D wave elevation the only set of random variables is the phase angle θ_{mn} (m=1…M, n=1…N). These random phase angles are assumed to be independent and each angle has the same uniform probability density function

$$p(\theta_{mn})=\begin{cases}1/2\pi, 0\le\theta_{mn}\le 2\pi\\ 0, otherwise\end{cases} \tag{4.2}$$

Thus the wave model represents a superposition of these wave components with different amplitudes, wave numbers, wave frequencies, and phase angles. It should be pointed out that the specifications of the wave components are carried out by two independent wave parameters k_m and ϕ_n, so that the superposition is accomplished by the double summation over m and n. The frequency ω_m related to the wave number k_m by dispersion equation. Amplitude α_{mn} is determined from the power spectrum of wave elevation as

$$\alpha_{mn}=\sqrt{2S_{\eta\eta}(\omega_m)\Delta\omega} \tag{4.3}$$

where $S_{\eta\eta}(\omega_m)$ is the power spectrum value corresponding to ω_m, and $\Delta\omega$ is the frequency interval.

Equation (4.1) can be easily written as 2-D wave as

$$\eta(x,t) = \sum_{m=1}^{M} \alpha_m \cos(k_m x - \omega_m t + \theta_m) \tag{4.4}$$

Wave kinematics are calculated from (4.5)—(4.8)

$$u(x,t) = \sum_{m=1}^{M} \omega_m \alpha_m \frac{\cosh(k_m y)}{\sinh(k_m d)} \cos(k_m x - \omega_m t + \theta_m) \tag{4.5}$$

$$\dot{u}(x,t) = \sum_{m=1}^{M} \omega_m^2 \alpha_m \frac{\cosh(k_m y)}{\sinh(k_m d)} \sin(k_m x - \omega_m t + \theta_m) \tag{4.6}$$

$$v(x,t) = \sum_{m=1}^{M} \omega_m \alpha_m \frac{\sinh(k_m y)}{\sinh(k_m d)} \sin(k_m x - \omega_m t + \theta_m) \tag{4.7}$$

$$\dot{v}(x,t) = \sum_{m=1}^{M} \omega_m^2 \alpha_m \frac{\sinh(k_m y)}{\sinh(k_m d)} \cos(k_m x - \omega_m t + \theta_m) \tag{4.8}$$

where *u* is horizontal water particle velocity, *v* is vertical water particle velocity, and *d* is the water depth.

Morison force model (Sarpkaya and Isaacson 1981) is

$$f = \frac{1}{2} C_D \rho A (u - \dot{x}) |u - \dot{x}| + C_M \rho V \dot{u} - C_A \rho V \ddot{x} \tag{4.9}$$

where $\dot{x}$ is horizontal velocity of the structure and $\ddot{x}$ is horizontal acceleration of the structure, C_D is the drag coefficient, C_M is the inertial coefficient, and C_A is the added mass coefficient. In the equation above, current is neglected.

4.3 Offshore System Identification in Frequency Domain based on GA

4.3.1 System Identification in Frequency Domain

Forward analysis in time domain is introduced in section **4.2**. However, since Morison force is not measurable, the time domain method has no advantage over frequency domain method, though it can include all the nonlinear phenomenon in hydrodynamic aspect and structural aspect. It is possible to do the forward analysis in time domain and transform the signals to its spectrums. However, in order to obtain spectrum with high resolution long time simulation (3 hours simulation as recommended in SNAME 5-5A (1997)) with small time steps is needed. Thus the time domain approach is not preferred. Hence, it is firstly assumed that the structure is linear. The dynamic equation of the SDOF mass system in time domain is

$$(M + C_A \rho dV)\ddot{x} + C\dot{x} + Kx = C_M \rho dV\dot{u} + \frac{1}{2} C_D \rho (dA)(|u|u - 2|u|\dot{x}) \qquad (4.10)$$

where M is structural mass, C is structural damping, K is structural stiffness, ρ is water density, dV is volume per length, dA is area per length, $\dot{u}, u$ are known by Airy wave theory from JONSWAP spectrum (Hs=11m, Tp=14.93) (Hasselmann *et al*., 1973).

Assume $$y_{in} = C_M \rho dV\dot{u} + \frac{1}{2} C_D \rho (dA)(|u|u - 2|u|\dot{x}) \qquad (4.11)$$

Equation (4.10) becomes $(M + C_A \rho dV)\ddot{x} + C\dot{x} + Kx = y_{in}$

Power spectrum of y_{in} ($S_{yy}(\omega)$) and power spectrum of x ($S_{xx}(\omega)$) are obtained from Fast Fourier Transform (FFT). In principle, not only the structural coefficients can be identified, but also the hydrodynamic coefficients. However, in order to demonstrate our strategy clearly the hydrodynamic coefficients are assumed to be known first. The frequency domain formulation of dynamic equation (4.10) is

$$S_{xx}(\omega) = |H(\omega)|^2 S_{yy}(\omega) \qquad (4.12)$$

where $$H(\omega) = \frac{1}{-\omega^2 (M + C_A \rho dV) + j\omega C + K} \qquad (4.13)$$

The fitness value in GA is calculated from

$$fitness = \sum_{i=1}^{n} (S_{xx}(\omega_i) - S_{measured}(\omega_i))^2 \qquad (4.14)$$

Normally the random wave elevation is defined by Gaussian distribution. The probability density distribution of structural response does not remain Gaussian, because the drag force term is quadratic, even though the structural system is linear. Thus up to second order spectrum (variance) may not be enough to describe dynamic structural response in detail. But it is good enough to serve the purpose of identification as demonstrated in the following example.

For further application hydrodynamic coefficients C_A and C_D are identified at the same time. The system is regarded as one which has two inputs y_1 and y_2 as equation follows.

$$y_1 = \dot{u} \tag{4.15}$$

$$y_2 = |u|u - 2|u|\dot{x} \tag{4.16}$$

The frequency domain formulation of (4.11) becomes

$$S_{xx}(\omega) = H_1^*(\omega)H_1(\omega)S_{y_1}(\omega) + H_1^*(\omega)H_2(\omega)S_{y_1y_2}(\omega) + H_2^*(\omega)H_1(\omega)S_{y_2y_1}(\omega) + H_2^*(\omega)H_2(\omega)S_{y_2}(\omega) \tag{4.17}$$

where $H_1(\omega) = \frac{H}{C_M \rho dV}$, $H_2(\omega) = \frac{2H}{C_D \rho dA}$ and $(*)$ means complex conjugate.

4.3.2 SDOF Identification of Mass, Stiffness and Damping.

As shown in Fig.4.2, the water depth of the sea is 100 m. The SDOF mass-spring system is 10 meter under the mean level surface of the sea. No current is considered. The random elevation is defined by JONSWAP spectrum (Fig.4.3). During 1 hour's observation, significant wave height is 11 m, and peak period is 15 s. The exact mass is 1000 kg, stiffness is 2467.4 N/m and damping ratio is 0.05.

As seen in Table 4.1, the absolute mean errors of stiffness and mass are only 0.11% and 4.49%, respectively. The identification error of damping is high simply because the spectral density is not sensitive to small change of damping ratio. If I/O signals are contaminated with 10% noise, the results also do not change much. In this case, the absolute mean errors of stiffness and mass are only 0.18% and 4.64% respectively.

From this example, it can be concluded that stiffness and mass can be identified with excellent accuracy by the proposed frequency-domain method using GA.

4.3.3 MDOF System Identification

The framework of substructural modal identification method as shown in Fig 2.2 can

still work for MDOF system identification in frequency domain. A tiny difference is in previous chapters time history is used to identify modal parameters, while power spectrum of the modal force and modal response is used in each mode to identify modal parameters here. Fast Fourier Transform (FFT) is employed to obtain signal power spectrum. Frequency domain formulation of dynamic equation in each mode is used.

An offshore platform is modeled as a 10-DOF lumped mass system (Fig 4.4). Its base is 90 meters under mean sea level. The levels of the first to ninth masses are 75, 65, 55, 45, 35, 25, 15 and 5 m, respectively, under the mean sea level. The tenth mass is 5 m above mean sea level. Exact value of each mass is 1000 kg except 10^{th} mass (3000 kg). The exact value of each stiffness is 2000 N/m. In addition, C_m=2, C_d=1.5 and each mass has a volume of $\pi/16$ m^3 with a cross-section area of 0.5 m^2 in the direction of wave propagation. Damping ratio of 0.05 is adopted. The random elevation is defined by JONSWAP spectrum (Fig.4.3). During 1 hour's observation, significant wave height is 11m, peak period is 15 s.

A substructure as demonstrated in Fig 4.4 is to be identified. Initial guess of each stiffness is 4000 N/m (double the exact value). Identification is conducted in frequency domain in every mode using the substructural modal identification method. The only difference from the numerical studies in Chapter 3 is that here power spectrum is used to calculate fitness values in GA (equation (4.14)) while time history is employed to

calculate fitness values in Chapter 3 (equation (2.10)). In the case of full measurement and zero noise, mean absolute error is 4.20%. When the signals are contaminated with 10% noise, the mean absolute errors are 4.04%, 4.07%, 4.29% and 5.44% in the cases of full measurement, 3/4 measurement (accelerations on levels 6, 7 and 8 are measured, except interface measurements) , 1/2 measurement (accelerations on levels 6 and 7 are measured) and 1/4 measurement (accelerations on level 6 are measured). In addition, it is found that maximum absolute errors are 4.24%, 4.58%, 5.69% and 7.90% respectively. It is found that proposed method performs very well in the case of noisy signals and incomplete measurement. Meanwhile, maximum absolute errors are relatively lower than those in numerical study of Chapter3.

In the case of full measurement and 3/4 measurement with 10% noise, the mean absolute error are slightly smaller than that in the case of full measurement with zero noise. This is due to the probabilistic nature of GA. Meanwhile, it shows that power spectrum is not sensitive to white noise.

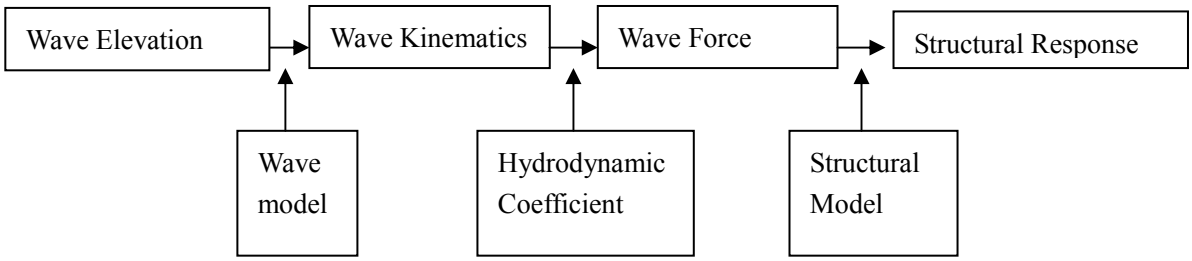

Fig.4.1 Offshore Structural Analysis Flow Chart

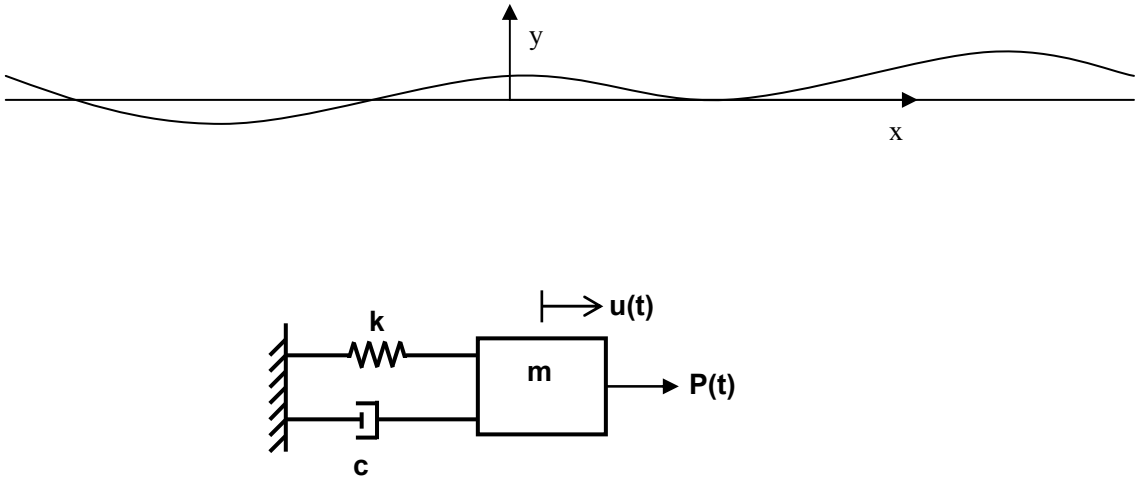

Fig.4.2 SDOF Mass-Spring System under Wave Force

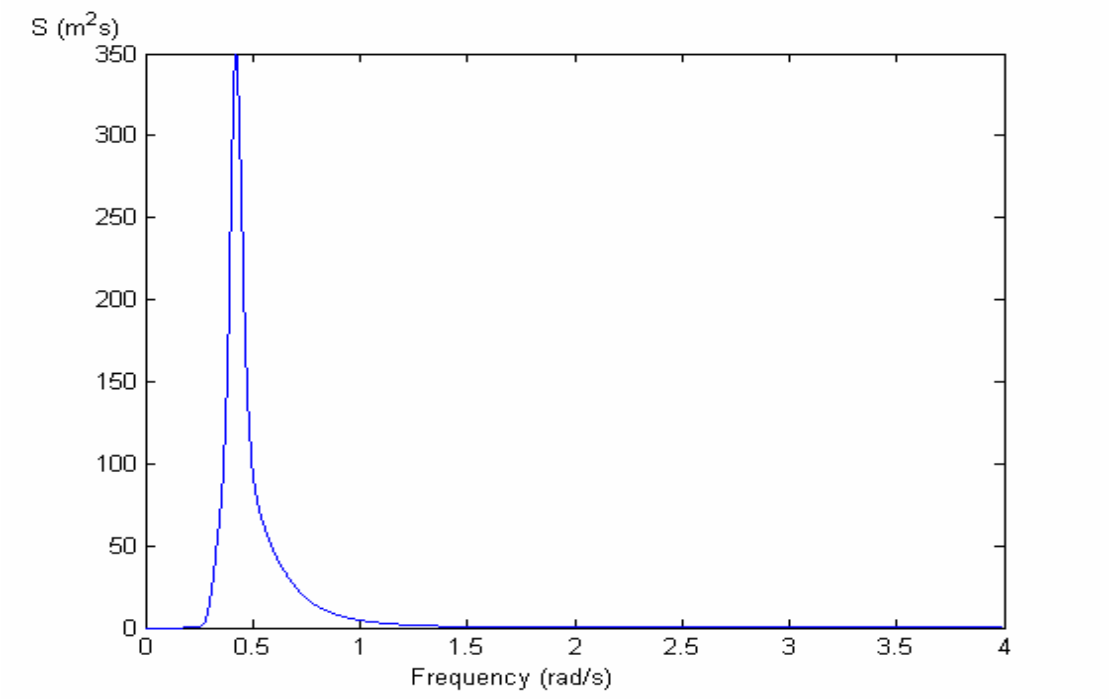

Fig.4.3 JONSWAP Spectrum

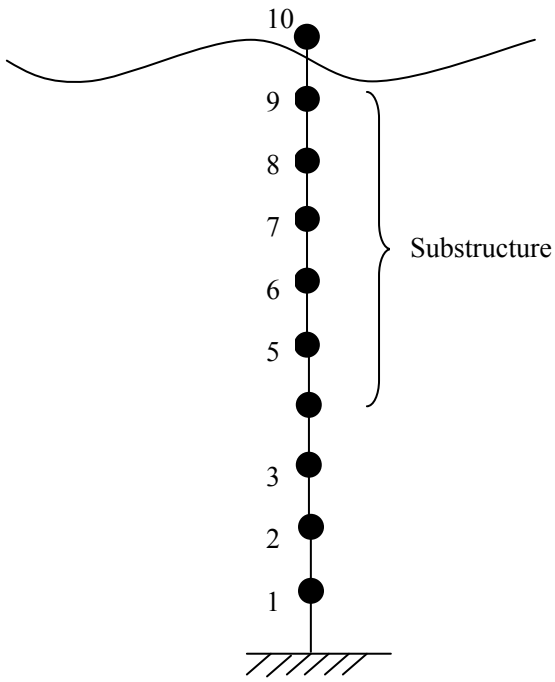

Fig 4.4 Offshore Platform MDOF Model

Table 4.1 Exact Values and Identified Values of SDOF Stiffness, Damping and Mass

	K(N/m)	C(Ns/m)(damping ratio)	M(KG)
Exact Value	2467.4	157.07(0.05)	1000
Identified Value (No noise)	2470.2	314.1(0.09)	1044.9
Absolute Mean Error	0.11%	99.99%	4.49%
Identified Value (10% noise)	2471.8	313.98(0.09)	1046.4
Absolute Mean Error	0.18%	99.90%	4.64%

Table 4.2 Identified Value of Substructure Stiffness of MDOF Offshore Platform

Number of Level	Exact Value	Identified Results				
		No Noise Full Measurement	10% Noise Full Measurement	10% Noise 3/4 Measurement	10% Noise 1/2 Measurement	10% Noise 1/4 Measurement
5	2000	2077.3	2084.7	2091.5	2113.7	2060.3
6	2000	2089.4	2084.5	2078.6	2063.8	2157.9
7	2000	2085.1	2065.0	2067.6	2073.1	2109.5
8	2000	2090.4	2084.8	2078.1	2064.4	2155.4
9	2000	2077.5	2084.6	2091.6	2113.7	2060.5
Absolute Mean Error		4.20%	4.04%	4.07%	4.29%	5.44%
Absolute Max Error		4.52%	4.24%	4.58%	5.69%	7.90%

CHPATER 5 CONCLUSIONS AND RECOMMENDATIONS

5.1 Conclusions

5.1.1 Substructural Modal Identification

In Chapter 2, a divide-and-conquer strategy is formulated on two fronts: (a) the large structural system for identification is physically divided into much smaller substructures in terms of number of DOFs and unknowns, and (b) the physical problem is transformed into modal domains with even lesser unknowns and recovered by exploiting the orthogonality properties.

1 Proposed method is shown to be fairly accurate and robust under the influence of incomplete measurements and I/O noise.

It is observed that substructural modal identification method performs well in the cases of incomplete measurement and noise (up to 10%) contaminated I/O data. The results are satisfactory in the worst situation. In terms of computing time, GA may not be the fastest algorithm. For example, least square method may finish the same identification task as example.3.1 in around 20 seconds. However, for this gradient based method, the noise tolerance cannot beyond 1%. Therefore, from the practical point of view, GA is more robust and applicable.

2 Proposed method can accelerate the convergence rate dramatically

Faster convergence compared with ordinary GA based method is another important feature of substructural modal identification method. It consumes far less than the direct GA. In section 3.4, identification of a 35 DOF substructure takes only about 30% of the direct substructural method. Therefore, it makes the identification of very large system practical. In addition, it is noticed that accuracy of identification results are not affected obviously by the size of the substructures, on the same level of noise signals and availability of measurement.

5.1.2 Application in Offshore Structural Identification in Frequency Domain

In section 4.3, offshore system identification is conducted on SDOF and MDOF system. Substructural modal identification method is used in the second example. From the results it is discovered that this method in frequency domain is not sensitive to noise. This should be due to the fact that the change of power spectral density is not sensitive to white noise. In addition, the maximum absolute error remains small compared with mean absolute error in MDOF example. It can be concluded that substructural modal identification method works pretty well in frequency domain. However, it is also observed that damping parameter identification is problematic in this study, though it is stated in Chapter 1 that damping identification is not included as a main purpose of this study. It stimulates a direction of future research work.

5.2 Recommendations on Future Work

(a) Measurement Unavailability

As the element components of physical model becomes complex, some measurements like nodal rotations is hard to be obtained. When they are treated as interface measurements, Koh and Shankar (2003c) provided a method which can solve this kind of problem in frequency domain. Future more complicated situations are to be considered.

(b) Criteria Optimization

As shown in the examples, damping ratio is very difficult to be identified accurately, if it is possible. It is found that the power spectrum is not sensitive to the change of damping ratio at all. This indicates that the sensitivity of the optimization criteria to the change of parameter being identified is a vital issue in system identification techniques. It is necessary to do a theoretical and numerical study on this aspect.

(c) Nonlinear problem of the structural & structural foundation model

Nonlinear phenomenon of structures like P-delta effect and foundation stiffness is identified in several literatures. However, P-delta effect is only mentioned in time domain analysis. The structural foundation stiffness is found to be linear in the ambient wave environment. Only during the storm period, nonlinearity is observed. Thus it can be assumed linear in certain sea state condition.

(d) Experiment verification

Real time history record will be collected from a Jacket or Jack-up platform. Proposed methodology will be employed to identify the real structure. This experiment also provides a verification of the proposed method.

REFERENCES

Barltrop N.D.P. and Adams A.J. (1991). *Dynamics of Fixed Marine Structures* (Third Edition), Butterworth Heinemann/ The Marine Technology Directorate Ltd.

Bathe K.J. (1996). *Finite Element Procedures*, Prentice-Hall, Englewood Cliffs, N.J.

Caravani. B., Watson M.L., and Thomson, W.T.(1977). "Recursive least-sqaures time domain identification of structural parameters." *J. Appl. Mech.*, 44, 135-40.

Carmichae D.G.. (1979). "The state estimation problem in experimental structural mechanics." *Proc. 3rd Int. Conf. on Application of Statistics and Probability in Soil and Struct. Engrg,* Sydney, Australia, 802-15.

Chassiakos, A. G., Kosmatopoulos, E. B., Masri, S. F., and Smyth, A. W. (1998). "Robust neural control of unknown structures." *Proceedings of ASCE 12th Engineering Mechanic Conference*, 17-20.

Chassiako AG, Masri SF. (1996). "Modeling unknown structural systems through the use of neural networks." *Earthquake Eng. Struct. Dyn.*, 25, 117-28.

Chou J.H., Ghaboussi, J. (2001). "Genetic algorithm in structural damage detection." *Comput. Struct.* , 79, 1335-353.

Doyle J.F. (1994). "A genetic algorithm for determining the location of structural impacts." *Experimental Mech.*, 34, 37-44.

Doyle, J.F. (1995). "Determining the size and location of transverse cracks in beams." *Experimental Mech.*, 35, 272-80.

Donley, M. G., and Spanos, P. D. (1990). "Introduction to statistical quadratization with applications to compliant offshore structures." *Springer-Verlag Lecture Notes in Engineering*, New York, N.Y.

Dunn, S.A. (1998). "The use of genetic algorithms and stochastic hill climbing in dynamic finite element model identification." *Compt. Struct.*, 66(4), 489-497.

Goldberg, D. (1989). *Genetic algorithms in search, optimization and machine learning*, Addison-Wesley, Reading, MA.

Hasselmann, K., Barnett, T.P., Bouws,E., Carlson, H., Cartwright, D.E., Enke, K., Ewing, J.A. ,Gienapp, H., Hasselmann, D.E., Kruseman, P., Meerburg, A., Mller, P. , Olbers, D.J. , Richter, K., Sell, W. , and Walden. H. (1973). "Measurements of wind-wave growth and swell decay during the Joint North Sea Wave Project (JONSWAP)." *Ergnzungsheft zur Deutschen Hydrographischen Zeitschrift Reihe* A(8) (Nr. 12), 95.

Hoshiya, M., and Maruyama, O. (1991). "Adaptive identification of autoregressive process." *J. Engrg. Mech.*, ASCE, 113(6), 813-824.

Hoshiya M., Satio E. (1984). "Structural identification by extended kalman filter." *J. Engrg. Mech.*, ASCE, 110(12), 1757-770.

Kareem, A., and Zhao, J. (1994). "Stochastic response analysis of tension leg platforms: A statistical quadratization and cubicization approach." *Proc., 13th Int. Conf. on Offshore Mech. And Arctic Engrg.* (OMAE 94), ASME, New York, N.Y., 281-292.

Karunakaran, D., Gudmestad,O.T., and Spidsoe, N. (1992). "Nonlinear dynamic response analysis of dynamically sensitive slender offshore structures." *Proc., 11th Int. Conf. on Offshore Mech. And Arctic Engrg.*(OMAE-92), ASME, New York, N.Y., 1A, 207-214.

Kitagawa, G. (1996). "Monte Carlo filter and smoother for non-Gaussian state space models." *J. Comput. Graph. Stat.*, 5(1), 1-25.

Koh, C.G., See, L. M., and Balendra, T. (1991). "Estimation of structural parameters in time domain: A substructure approach." *Earthquake Eng. Struct. Dyn.*, 20, 787-801.

Koh, C. G., See, L. M., and Balendra, T. (1995). "Identification and uncertainty estimation of structural parameters." *Engrg. Struct.*, 17(3), 179-186.

Koh C.G., Hong, B. and Liaw,C.Y. (2000). "Parameter identification of large structural systems in time domain." *J. Struct. Engrg.*, 126(8), 957-63.

Koh C.G., Hong, B. and Liaw, C.Y. (2003a). "Substructural and progressive structural

identification methods." *Engrg. Struct.*, 25,1551-1563.

Koh C. G., Chen, Y. F., Liaw, C.-Y. (2003b). "A hybrid computational strategy for identification of structural parameters." *Comput. Struct.*, 81, 107-117.

Koh C. G., and Shankar, K.. (2003c). "Substructural identification method without interface measurement." *J.Engrg. Mech.*, 129(7), 769-776.

Kosmatopoulos EB, Polycarpou MM. (1995). "High-order neural network structures for identification of dynamical systems." *IEEE Trans Neural Networks*, 6(2), 422-31.

Loh, C. H., and Tsaur, Y. H. (1998). "Time domain estimation of structural parameters." *Engrg. Struct.*, 10, 95-105.

Oreta, W. C., and Tanabe, T. A. (1994). "Element identification of member properties of framed structures." *J. Struct. Engrg.*, ASCE, 120(7), 1961-1976.

Perry, M. J., Koh, C. G. and Choo, Y. S. (2006). "Modified genetic algorithm strategy for structural identification". *Comput. Struct.*, 84, 529-540.

Pierson, W.J., and Holmes, P. (1965). "Irregular wave forces on a pile." *J. Wtrwy. And Harb. Div.*, ASCE, 91(4),1-10.

Sarpkaya, T. and Isaacson, M. (1981). "Mechanics of Wave Forces on Offshore Structures." *Van Nostrand Reinhold*, New York, NY.

Sato, T., and Kaji, K. (2000). "Structural system identification using Monte Carlo filter." *3rd US-Japan workshop on nonlinear system identification and structural health monitoring*.

SNAME T&R 5-5A.(1997). *Site specific assessment of mobile jack-up units.* 1st Edition – Rev 1. Society of Naval Architects and Marine Engineers, New Jersey.

Spanos, P.D., and Donley, M.G. (1991). "Equivalent statistical quadratization for nonlinear system." *J. Engrg. Mech.*, ASCE, 117(6), 1289-1310.

Tickell, R.G. (1977). "Continuous random wave loading on structural members." *The*

Struct. Engr., 55(6), 209-222.

Wu X, Ghaboussi J, and Garrett JH. (1992). "Use of neural networks in detection of structural damage." *Comput. Struct.*, 42, 649-59.

Yun C.B., Bahng EY. (2000). "Substructural identification using neural networks." *Comput.Struct.*, 77(1), 41-52.

Yun C.B., Kim W.J. and Ang A. H. S. (1988). "Damaged assessment of bridge structures by system identification." *Proc. Korea-Japan Joint Seminar on Emerging Technol. In Struct. Engrg. And Mech.*, 182-93.

Yun, C. B., and Lee, H. J. (1997). "Substructural identification for damage estimation of structures." *Struct. Saf.*, 19(1), 121-140.

Yun C.B., and Shinozuka M. (1980). "Identification of nonlinear structural dynamic system." *J. Struct. Mech.*, 8(2), 187-203.

Yoshida, I. (2000). "Damage detection by using Monte Carlo filter with non-Gaussian Noise." *3rd US-Japan workshop on nonlinear system identification and structural health monitoring*.

APPENDIX A GENETIC ALGORITHM PROCEDURE

Genetic algorithm is inspired by Darwin's theory of evolution. Solutions are evolved in this algorithm. This algorithm is started with a set of initial solution (guessed) which are called population. One population is taken to generate the next population. It is hoped that the next generation will be better than current generation. Thus solutions with higher fitness will have more chance to give offspring. In this way, the population evolves. Finally we have the results according to some convergence criteria.

Outline of the basic genetic algorithm:

1 *Start* Generate random population of *n* chromosomes (suitable solutions for the problem).

2 *Fitness* Evaluate the fitness value of each chromosome in this population.

3 *New population* Create a new population by repeating following steps until the new population is complete.

a. *Selection* Select two parent chromosomes from a population according to their fitness (the better fitness, the bigger chance to be selected).

b. *Crossover* With a crossover probability crossover the parents to form a new offspring (children). If no crossover was performed, offspring is an exact copy of parents.

c. *Mutation* With a mutation probability mutate new offspring at each locus (position in chromosome).

d. *Accepting* Place new offspring in a new population.

4 *Replace* New generated population for a further run of algorithm.

5 *Test* If the end condition is satisfied, stop, and return the best solution in current population.

6 *Loop* Go to step 2.

Above procedure is demonstrated in Fig A2. Definitions of floating GA operators are described as follows:

Roulette Wheel Selection

$$p(i) = \frac{f(i)}{\sum_{i=1}^{N} f(i)} \tag{A1}$$

where $p(i)$ is the probability of being selected of ith individual chromosome, $f(i)$ is the fitness value of ith individual chromosome, N is the total population number in each generation.

Arithmetic Crossover

$$c1 = \alpha a + (1-\alpha)b \tag{A2}$$

$$c2 = \alpha b + (1-\alpha)a \tag{A3}$$

where *a, b* are two parents, *c*1 and *c*2 are two children chromosome. α is a random value generated uniformly between 0 and 1.

Heuristic Crossover

Heuristic crossover can make the population go towards the best solution through the fastest direction. Detail description: Using two parameter vectors, *a* and *b*, (*a* with higher fitness value) compute *c*1 = α (*a* - *b*) + *a*. If *c*1 satisfies all constraints, use it. Otherwise choose another α value and repeat. Set *c*1 equal to the better of *a* and *b* if a satisfactory mixed *c*1 is not found by a preset number of attempts. In this fashion produce *c*2.

Non-uniform Mutation

$$C_1^{'} = (1-p)C_1 + p * lb \quad \text{(50\% probability)} \tag{A4}$$

$$C_1^{'} = (1-p)C_1 + p * ub \quad \text{(50\% probability)} \tag{A5}$$

where $p = (1 - j / gn)^B rand$, j is the index number of the current generation, *gn* is the total generation number, *B* is constant, *rand* is a number chosen from a uniform distribution on the interval (0.0,1.0). *lb* and *ub* are the low bound and upper bound of the chosen parameter respectively. This mutation connected the parameters with the upper or lower bound randomly.

Whole Non-uniform Mutation

Non-uniform mutation on all parameters.

Uniform Mutation

Randomly change a parameter in its search range with uniform probability.

Creep Mutation

Creep mutation is a kind of mutation according to Gaussian distribution. This mutation is used on the individual chromosomes with relatively high fitness value in order to accelerate the convergence.

Fitness Calculation

GA and all other evolutionary optimization techniques are particularly useful in situations in which it is easy to determine the quality of a single solution, but hard to go through all possible solutions one by one.

To define quality, fitness value plays a vital important role in whole GA search procedure. It is the criteria of judging the quality of the searched result. Usually this is defined in a least square manner, as equation (A6).

$$\sum_{i=1}^{k} W(i)\left(\ddot{u}_{ip} - \ddot{u}_{im}\right)^2 \qquad \text{(A6)}$$

where $\ddot{u}_{ip}$ is the acceleration output as predicted, $\ddot{u}_{im}$ is the acceleration output as measured, $W(i)$ is weight function. This is a typical definition of fitness. GA is a method to minimize the fitness function in an optimization point of view. A fitness landscape is shown in Fig.A1.

Actually speaking, GA is a well structured algorithm. Moreover, each operator has various versions of fulfillment corresponding to different practical problem. Thus before a researcher or engineer apply GA to solve his problem, what he needs to do is to formulate his own GA flowchart as the most powerful and efficient GA to his usage. This process of course needs tedious "code tuning" and numerous time and energy. However, the outcome will prove its worthy payback. In the next part, the detailed structure of GA used in this study is presented.

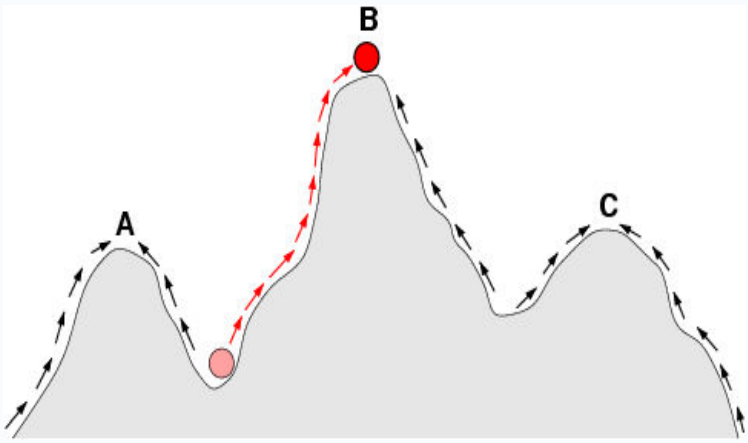

Fig A1 Sketch Of a Fitness Landscape. The arrows indicate the preferred flow of a population on the landscape, and the points A, B, and C are local optima. The ball indicates a population that moves from a very low fitness value to the top of a peak.

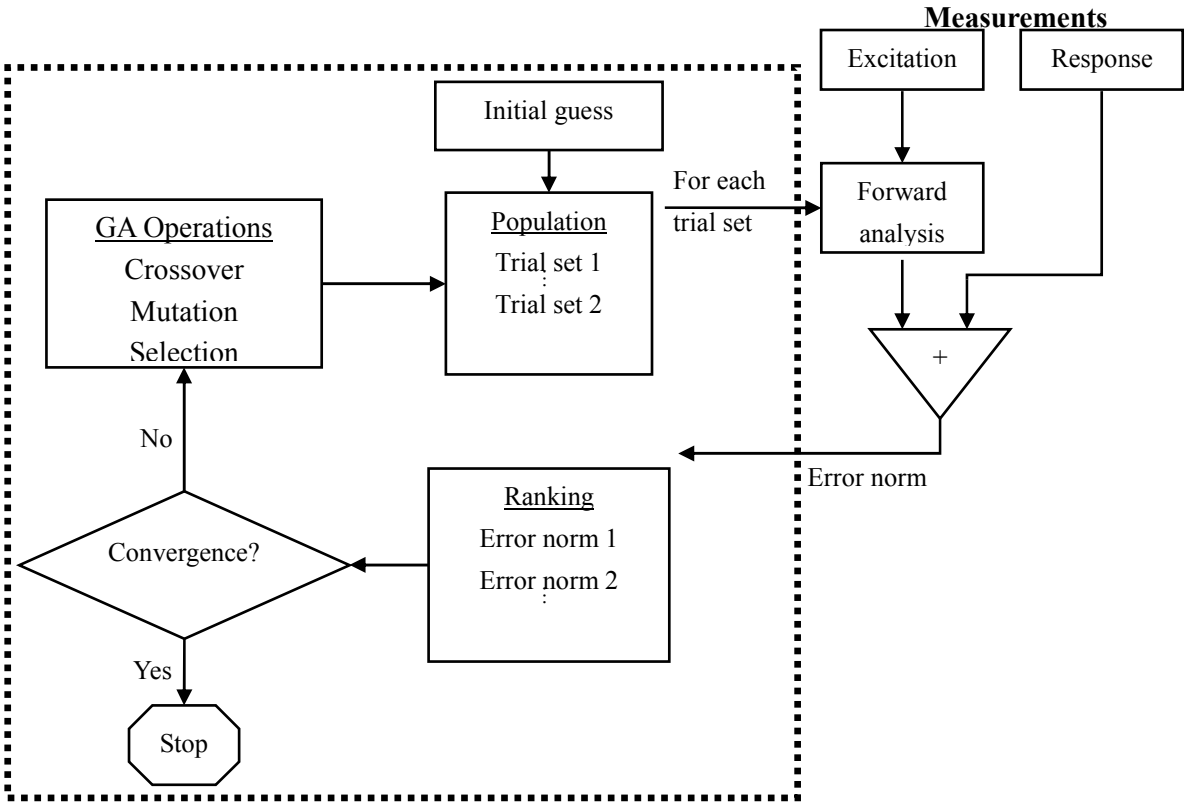

Fig A2 Direct GA Flow Chart

APPENDIX B MATLAB CODE LIST

B1 Function to formulate substructure matrix

```
%for the substructure consisting of element:10 11 12 13 14 15 16 17 18 19 20
%Truss Example
function[sGMr,sGMj,sGKr,sGKj,r,sGCr,sGCj,a,b,Kcoef,ok]=trusssubstiffmatrix(po
ph,noe,Nnoe)
%noe is the element number of the substructure extracted
%E=200e6; % Youngth modul
A=0.0015;% crosssection area

subAss=[2 4;1 4;1 3;3 4;4 6;3 6;3 5;5 6;6 8;5 8;5 7];
%connective array
subCo(:,1)=subAss(:,1)*2.-1;
subCo(:,2)=subAss(:,1)*2;
subCo(:,3)=subAss(:,2)*2-1;
subCo(:,4)=subAss(:,2)*2;
load X;%x coordinate of all nodes
load Y;%y coordinate of all nodes
subX=X(5:12);subY=Y(5:12);
dens=7.850% density of material
EM=zeros(4,4,Nnoe);EK=zeros(4,4,Nnoe);
%~~~~~~~~~~~~~~~~~~~~~~~~~~~~~~~~~`formulate element stiffness matrix and
element mass matrix

for i=1:Nnoe
    X1=subX(subAss(i,1));X2=subX(subAss(i,2));%x coordinate
    Y1=subY(subAss(i,1));Y2=subY(subAss(i,2));%y coordinate
    L=sqrt((X2-X1)^2+(Y2-Y1)^2);% element length
    C=(X2-X1)/L;%cos
    S=(Y2-Y1)/L;%sin
    EM(:,:,i)=(dens*A*L/6)*[2*C^2 2*C*S C^2 C*S;2*C*S 2*S^2 C*S S^2;C^2
C*S 2*C^2 2*C*S;C*S S^2 2*C*S 2*S^2];%Element mass matrix
    EK(:,:,i)=(poph(i)/L)*[C^2 C*S -C*C -C*S; C*S S*S -C*S -S*S;-C*C -C*S
C*C C*S;-C*S -S*S C*S S*S];%element stiffness matrix
    Kcoef(:,:,i)=(1/L)*[C^2 C*S -C*C -C*S; C*S S*S -C*S -S*S;-C*C -C*S C*C
C*S;-C*S -S*S C*S S*S];%coefficient matrix
end
```

```
subGK=zeros(2*size(subX,2),2*size(subX,2));
subGM=zeros(2*size(subX,2),2*size(subX,2));
ok=zeros(8,8,Nnoe);
for e=1:size(subAss,1)
    for i=1:4
        for j=1:4
            subGK(subCo(e,i),subCo(e,j))=
subGK(subCo(e,i),subCo(e,j))+EK(i,j,e);
            subGM(subCo(e,i),subCo(e,j))=
subGM(subCo(e,i),subCo(e,j))+EM(i,j,e);
            if subCo(e,i)>=5&subCo(e,i)<=12
                if subCo(e,j)>=5&subCo(e,j)<=12

ok(subCo(e,i)-4,subCo(e,j)-4,e)=ok(subCo(e,i)-4,subCo(e,j)-4,e)+Kcoef(i,j,e);
                end
            end
        end
    end
end

load force
Fr=force(13:20,:);
%~~~~~~~~~~~~~~~~~~~~~~~~~~~~~~~~~~~~~~~~~~~~~~~~~~divide interface
matrix and core matrix
sGKj=[subGK(5:12,1:4) subGK(5:12,13:16)];sGMj=[subGM(5:12,1:4)
subGM(5:12,13:16)];
sGKr=subGK(5:12,5:12);sGMr=subGM(5:12,5:12);
load acceler1;
mdata=[acceler1(7:10,:);acceler1(19:22,:)];%the order of the acceleration is after
extracting the displacement boundary condition
accj=mdata;

r=-inv(sGKr)*sGKj;
%~~~~~~~~~~~~~~~~~~~~~~~~~~~~~~~~~~~dynamic response neglecting interface
damping sGMr*ddu+sGCr*du+sGKr*u=Fr-(sGMj+sGMr*r)dduj/Newmark Method
sGCr=poph(Nnoe+1)*sGMr+poph(Nnoe+2)*sGKr;
a=poph(Nnoe+1);b=poph(Nnoe+2);
```

B2 Function of eigenvalue analysis

```
function [A,B]=subsuper(K,M,y)
x(:,:,1)=y;
[m,n]=size(y);
for i=1:1000
    xg(:,:,i+1)=inv(K)*M*x(:,:,i);
    x(:,1,i+1)=xg(:,1,i+1)/sqrt(xg(:,1,i+1)'*M*xg(:,1,i+1));
    b(1,i+1)=1/sqrt(xg(:,1,i+1)'*M*xg(:,1,i+1));
    for j=2:n
        for k=1:j-1
            a(k,j)=xg(:,k,i+1)'*M*xg(:,j,i+1)/(xg(:,k,i+1)'*M*xg(:,k,i+1));
            xg(:,j,i+1)=xg(:,j,i+1)-a(k,j)*xg(:,k,i+1);
        end
        x(:,j,i+1)=xg(:,j,i+1)/sqrt(xg(:,j,i+1)'*M*xg(:,j,i+1));
        b(j,i+1)=1/sqrt(xg(:,j,i+1)'*M*xg(:,j,i+1));
    end
    c=abs((b(:,i+1)-b(:,i))./b(:,i+1));
    if max(c)<=1e-6
        break
    end
end

A=x(:,:,i+1);
for k=1:n
    B(k)=x(:,k,i+1)'*K*x(:,k,i+1)/(x(:,k,i+1)'*M*x(:,k,i+1));
end
```

B3 Function to recover physical parameters:

```
function [phyparec]=recover(eigve,DOF,Modapar,ok,Nnoe)
for i=1:DOF
      for e=1:Nnoe
      Ak(i,e)=eigve(:,i)'*ok(:,:,e)*eigve(:,i);
end
end
temp=DOF;
for i=1:DOF
      for j=(i+1):DOF

                  for e=1:Nnoe
                        Ak(temp+1,e)=eigve(:,i)'*ok(:,:,e)*eigve(:,j);
                  end

            temp=temp+1;
      end
end
Bk=zeros((DOF^2+DOF)/2,1)
Bk(1:DOF,1)=Modapar(:,1);
Xk=inv(Ak'*Ak)*Ak'*Bk;
phyparec=Xk';
phyparec(Nnoe+1)=mean(Modapar(:,2));
phyparec(Nnoe+2)=mean(Modapar(:,3));
```

B4 Function using Newmark method to calculate fitness value

```
function Mfit=Mfitf(P,Mmdata,Mpop,nofm,dt,Mn)
for j=1:50
      Mpoph=Mpop(j,:);
      Kn=Mpoph(1);
      a=Mpoph(2);
      b=Mpoph(3);
      Cn=a*Mn+b*Kn;
      M1=Mn+Cn*dt*0.5+Kn*dt*dt*0.25;
      M2=Cn*dt*0.5+Kn*dt*dt*0.25;
      C1=Cn+Kn*dt;
      n=size(Mmdata,2);
      Mmdatah=Mmdata(nofm,:);
      Ph=P(nofm,:);
      ddu=0;du=0;u=0;Mfit(j)=0;
for i=1:n-1
      ddu1=ddu;du1=du;u1=u;
      ddu=inv(M1)*(Ph(:,i+1)-M2*ddu1-C1*du1-Kn*u1);
      du=du1+dt*(ddu+ddu1)*0.5;
      u=du1*dt+(ddu+ddu1)*dt*dt*0.25+u1;
            w=sum(abs(ddu))./abs(ddu);
          % c=ddu+r*accj(:,i+1);
      Mfit(j)=Mfit(j)+sum(w.*(ddu-Mmdatah(:,i+1)).^2);
   end
Mfit(j)=1/Mfit(j);
end
```

B5 Main script of the substructural modal identification

```
%this is the main m-file for the structural parametric identification based on GA.
%in this file,at first the size of the popuation, the wanted number of generation, the probability of crossover and mutation
%are input. this file called functions for fitness calculation, selection, crossover and mutation.

%exact=('welcom to the structural identification simulation system, please input the first generation of the parameters:');
pn=50;%pn=input('please indicate the size of the population');
gn=20;%gn=input('please indicate how many generations you want');
load acceler1;
load force;
dt=0.01;
E=200e6; % Youngth modul
A=0.0015;% crosssection area
dens=7.850% density of material
noe=[10 11 12 13 14 15 16 17 18 19 20];Nnoe=size(noe,2);
exact(1:Nnoe)=E*A;exact(Nnoe+1)=0.00642;exact(Nnoe+2)=0.347;
ub=1.5*exact;
lb=0.5*exact;
accj=[acceler1(7:10,:);acceler1(19:22,:)];%the order of the acceleration is after extracting the displacement boundary condition
Pr=force(13:20,:);
mdata=[acceler1(6,:);acceler1(7,:);acceler1(9,:)];
phypar(1,:)=0.5*exact;
for conv=1:5
      for j=1:size(phypar,2)
            if phypar(conv,j)<lb(1,j)
                  phypar(conv,j)=lb(1,j);
    elseif phypar(conv,j)>ub(1,j)
                  phypar(conv,j)=ub(1,j);
            end
      end
      DOF=8;
[Mrr,Mrj,Krr,Krj,r,Crr,Crj,a,b,Kcoef,ok]=trusssubstiffmatrix(phypar(conv,:),noe,Nnoe);
%fabricate the stiff matrix of the substructure
for i=1:8;for j=1:8;y(i,j)=randn;end;end
[eigve,eigva]=subsuper(Krr,Mrr,y);%eigenvalue problem
[P,F]=modalexcit(Pr,Mrr,Mrj,r,accj,DOF,eigve);%calculate modal excitation
[Ua]=updataAct(mdata,Krr,Mrr,Krj,F,phypar,dt,DOF,nos,accj,localno,a,b,Crj,Crr,r);
%updata measured response(incomplete measurement)
```

```
[Mmdata]=modalresponse(Ua,Mrr,eigve,DOF); %calculate the modal response
[Modapar,bestfit,Mn1,avfit,best,Mpop]=modalGA(Ua,Mmdata,DOF,Krr,Mrr,Crr,P,e
igve,gn,a,b,dt);%estimate the modal parameters of each mode
bestfit1(:,:,conv)=bestfit;
Modapar1(:,:,conv)=Modapar;
avfit1(:,:,conv)=avfit;
[phyparec]=recover(eigve,DOF,Modapar,ok,Nnoe);
%recover the physical parameters from the modal parameter
phypar(conv+1,:)=phyparec;
err(conv)=mean(abs(phypar(conv+1,1:Nnoe)-phypar(conv,1:Nnoe))./abs(phypar(co
nv,1:Nnoe)));
    if err(conv)<0.05
        break
    end
end
pop=phypar;
    fit=fitness(nos,pop,dt,pn,accj,Pr,Mrr,mdata,localno,subn,F);
        for k=1:size(pop,1)
    if max(fit)==fit(k)
        break
  end
end
best=pop(k,:);
bestfit(j)=fit(k);
```

B6 Function to calculate modal excitation

```
function [P,F]=modalexcit(Pr,Mrr,Mrj,r,accj,DOF,eigve)
F=Pr-(Mrj+Mrr*r)*accj;
%f=Fr-(sGMj+sGMr*r)*accj;
for i=1:DOF
      P(i,:)=eigve(:,i)'*F;
end
```

B7 Function to calculate modal response

```
function [Mmdata]=modalresponse(Ua,Mrr,eigve,DOF)
%calculate the modal response(incomplete actual measurements are obtained through proportional rule)
Mn=eigve'*Mrr*eigve;
for i=1:DOF
      Mmdata(i,:)=eigve(:,i)'*Mrr*Ua/Mn(i,i);
end
```

B8 Function to update measurement when in the case of incomplete measurement

```
Function[Ua,c]=updataAct(mdata,Krr,Mrr,Krj,F,phypar,dt,DOF,nos,accj,localno,a,
b,Crj,Crr,r)%update measured response(incomplete measurement)

n=size(accj,2);
u=zeros(DOF,n);du=zeros(DOF,n);ddu=zeros(DOF,n);
M1=Mrr+Crr*dt*0.5+Krr*dt*dt*0.25;
      M2=Crr*dt*0.5+Krr*dt*dt*0.25;
      C1=Crr+Krr*dt;
for i=1:n-1
      ddu(:,i+1)=inv(M1)*(F(:,i+1)-M2*ddu(:,i)-C1*du(:,i)-Krr*u(:,i));
      du(:,i+1)=du(:,i)+dt*(ddu(:,i+1)+ddu(:,i))*0.5;
      u(:,i+1)=du(:,i)*dt+(ddu(:,i+1)+ddu(:,i))*dt*dt*0.25+u(:,i);
end
c=ddu+r*accj;
for i=1:DOF
Ua(i,2:n)=((mdata(1,2:n)./c(1,2:n)).*c(i,2:n)+(mdata(2,2:n)./c(3,2:n)).*c(i,2:n)+(m
data(3,2:n)./c(4,2:n)).*c(i,2:n))/3;
end
Ua(1,:)=mdata(1,:);
Ua(3,:)=mdata(2,:);
Ua(4,:)=mdata(3,:);
Ua=Ua-r*accj;
```